bioRxiv preprint doi: https://doi.org/10.1101/581504; this version posted March 18, 2019. The copyright holder for this preprint (which was not certified by peer review) is the author/funder, who has granted bioRxiv a license to display the preprint in perpetuity. It is made available under aCC-BY 4.0 International license.

# The parietal operculum preferentially encodes heat pain and not salience

Björn Horing, Christian Sprenger, Christian Büchel

Björn Horing, Ph.D. (corresponding author)
Affective Neuroscience Group
Department of Systems Neuroscience
University Medical Center Hamburg-Eppendorf
e-mail b.horing@uke.de
phone +49 040 7410 - 57890

Christian Sprenger, M.D.
Affective Neuroscience Group
Department of Systems Neuroscience
University Medical Center Hamburg-Eppendorf

Christian Büchel, M.D.
Affective Neuroscience Group
Department of Systems Neuroscience
University Medical Center Hamburg-Eppendorf

bioRxiv preprint doi: https://doi.org/10.1101/581504; this version posted March 18, 2019. The copyright holder for this preprint (which was not certified by peer review) is the author/funder, who has granted bioRxiv a license to display the preprint in perpetuity. It is made available under aCC-BY 4.0 International license.

**Abstract**

Substantial controversy exists as to which part of brain activity is genuinely attributable to pain-related percepts, and which activity is due to general aspects of sensory stimulation, such as its salience. The challenge posed by this question rests largely in the fact that pain is per se highly salient, a characteristic which therefore has to be matched by potential control conditions. Here, we used a unique combination of functional magnetic resonance imaging, behavioral and autonomic measures to address this longstanding debate in pain research.

Subjects rated perceived intensity in a sequence alternating between heat and sound stimuli. Neuronal activity was monitored using fMRI. Either modality was presented in six different intensities, three of which lay above the pain threshold (for heat) or the unpleasantness threshold (for sound). We performed our analysis on 26 volunteers in which psychophysiological responses (as per skin conductance responses) did not differ between the two stimulus modalities. Having thus ascertained a comparable amount of stimulus salience, we analyzed pain-related stimulus response functions, and contrasted them with those of the salience-matched acoustic control condition. Furthermore, analysis of fMRI data was performed on the brain surface to circumvent blurring issues stemming from the close proximity of several regions of interest located in heavily folded cortical areas. We focused our analyses on insular and periinsular regions which are strongly involved in processing of painful stimuli. We employed an axiomatic approach to determine areas showing higher activation in painful compared to non-painful heat, and at the same time showing a steeper stimulus response function for painful heat as compared to unpleasant acoustic stimuli. Intriguingly, an area in the posterior parietal operculum emerged whose response showed a pain preference, and where we can unequivocally exclude salience as explanation.

This result has important implications for the interpretation of functional imaging findings in pain research, as it clearly demonstrates that there are areas whose pain-related activity is not due to

bioRxiv preprint doi: https://doi.org/10.1101/581504; this version posted March 18, 2019. The copyright holder for this preprint (which was not certified by peer review) is the author/funder, who has granted bioRxiv a license to display the preprint in perpetuity. It is made available under aCC-BY 4.0 International license.

46 general stimulus characteristics such as salience. Conversely, several areas did not conform to the

47 formulated axioms to rule out general factors as explanations.

48

bioRxiv preprint doi: https://doi.org/10.1101/581504; this version posted March 18, 2019. The copyright holder for this preprint (which was not certified by peer review) is the author/funder, who has granted bioRxiv a license to display the preprint in perpetuity. It is made available under aCC-BY 4.0 International license.

## Introduction

Pain is a multidimensional experience, including sensory-discriminative, affective-motivational, cognitive-evaluative as well as motor components [1], and is defined as “an unpleasant sensory and emotional experience associated with actual or potential tissue damage, or described in terms of such damage” [2]. Following the advent of brain imaging, recurring patterns of brain activity following painful stimuli were summarized as a “pain matrix”, comprising primary and secondary somatosensory cortices, cingulate cortices, as well as the insular subregions, among other structures [3,4].

This activity has frequently been attributed to pain per se. However, it has been pointed out that precisely because pain is a composite sensation, some of the observed activation may or may not be exclusively pain-related [5,6]. These studies provided evidence that in many cortical regions, activation is observed for both painful and non-painful (such as tactile or auditory) stimuli. Hence, general processes such as stimulus salience were put forward as an alternative interpretation. These contributions have led to lively controversy [7–9]. Recently, the authors positing the initial challenge to the “pain matrix” concept revisited these issues [10], and reemphasized that great care should be taken experimentally to match non-painful control modalities , which has frequently been neglected in previous studies.

In addition to the question of stimulus salience, many experiments have relied on the use of single stimulus intensities to characterize neuronal responses, when using painful stimulation and compared these responses to a non-painful control condition. However, such approaches disregard the possibility of modality-specific baseline activation, further compounding the issue to properly account for nonspecific activation [11]. A possible solution is to employ multiple stimulus intensities, which allows for the characterization of modality-specific stimulus-response functions [12,13], and a comparison of these between modalities.

bioRxiv preprint doi: https://doi.org/10.1101/581504; this version posted March 18, 2019. The copyright holder for this preprint (which was not certified by peer review) is the author/funder, who has granted bioRxiv a license to display the preprint in perpetuity. It is made available under aCC-BY 4.0 International license.

Here, we address these issues, and present a novel approach that allows to directly test whether there are cortical regions that can be defined as salience detectors or show preferential pain processing. We employed heat and sound as stimulus modalities. Stimuli were presented in alternating modalities in a within-subjects design. Of each modality, we used six graded intensities – three below and three above the pain and unpleasantness threshold, respectively. This allowed us to determine stimulus-response functions of physical intensities or their percepts, and relate those to neuronal activity [12–14]. Importantly, auditory and thermal intensities were calibrated as equisalient using an objective autonomic measure (skin conductance responses; SCR) [15].

We paid particular attention to insular and periinsular regions, especially the posterior insula and the parietal operculum (the secondary somatosensory cortex), all of which have been reported as early components of pain-responsive cortical areas [4,9,16–18].

To define areas as preferentially pain-processing, our analyses followed an axiomatic approach which posits several logical conditions to be met to make a valid inference (see [19], for a similar approach in pain avoidance). Within this rigorous approach, we formulated the following set of conditions to preclude the possibility that activity in an area could be explained by salience alone: The effect of painful stimulation should be larger than that of non-painful heat (axiom 1); the effect of painful stimulation should be larger than that of (salience-matched) unpleasant sound (axiom 2); the relationship of ratings and BOLD should be stronger for painful heat than for non-painful heat (axiom 3); the positive relationship of pain ratings and BOLD responses should be stronger for painful heat than for (salience-matched) unpleasant sound (axiom 4).

bioRxiv preprint doi: https://doi.org/10.1101/581504; this version posted March 18, 2019. The copyright holder for this preprint (which was not certified by peer review) is the author/funder, who has granted bioRxiv a license to display the preprint in perpetuity. It is made available under aCC-BY 4.0 International license.

## Results

Heat stimuli were presented using a CHEPS thermode, sounds were 1kHz beeps presented binaurally via headphones. For a brief overview, see Figure 1. Details are provided in the Method section.

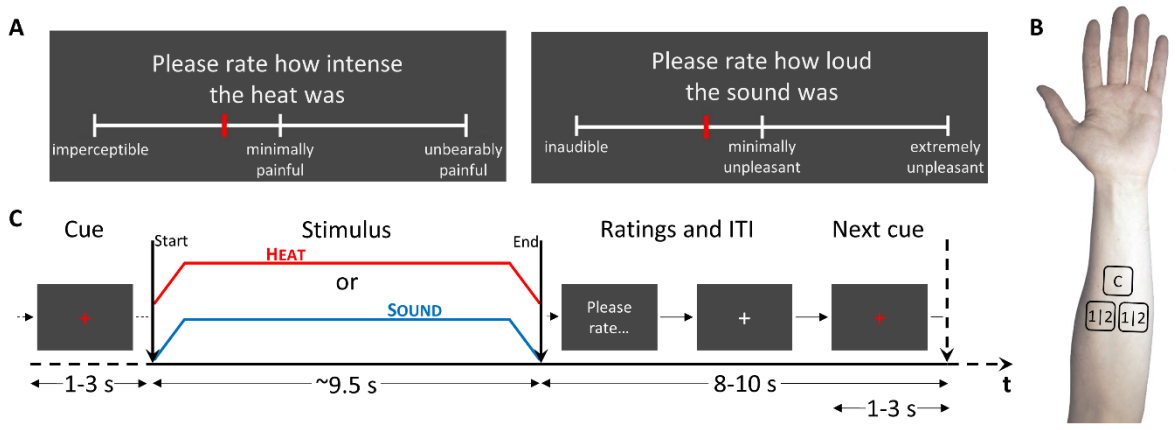


**Figure 1.** Experimental procedures. **A.** Visual analogue scales (VAS) for rating heat (left) and sound stimuli (right). The midpoint signifies the pain threshold, corresponding to a score of 0 in a conventional VAS. **B.** Thermode arrangement on a subject's forearm. Patch C was used for calibration, patches 1|2 were used in counterbalanced fashion for experimental sessions 1 and 2. **C.** Protocol by time. A visual cue (white fixation cross turning red) announced the upcoming stimulus (either heat or sound) and stayed visible throughout stimulation, which was 8 seconds at plateau (roughly 9.5 seconds all in all, depending on calibration). Subjects were then prompted to rate the stimulus. After rating, the white fixation cross reappeared, to turn red again for the next cue. Stimulus modalities were always alternating.

### *Sample*

A core prerequisite of our analysis strategy was that both modalities (heat and sound) were matched with respect to salience. Although previous studies based salience estimates on ratings, this can be problematic when comparing sound and heat stimuli due to differential scaling. We therefore selected skin conductance responses (SCR) as an objective readout parameter linked to salience [15,20,21]. Consequently, our approach is based on comparable SCR for sound and heat stimuli. This

bioRxiv preprint doi: https://doi.org/10.1101/581504; this version posted March 18, 2019. The copyright holder for this preprint (which was not certified by peer review) is the author/funder, who has granted bioRxiv a license to display the preprint in perpetuity. It is made available under aCC-BY 4.0 International license.

115 necessitated the selection of suitable subjects and experimental sessions that fulfilled this criterion
116 (see Methods). Analysis included N=26 subjects (50% female, mean age±SD 25.8±3.6; see S1 Table
117 for more detailed sample characteristics).

118

119 *Skin conductance results*

120 As intended by stimulus matching, no significant difference between modalities prevailed (p=0.177)
121 (random intercept model; Figure 2). SCR increased by intensity (t(308)=7.797, p=1e-13). There was
122 no interaction between intensity and modality (p=0.514).

123

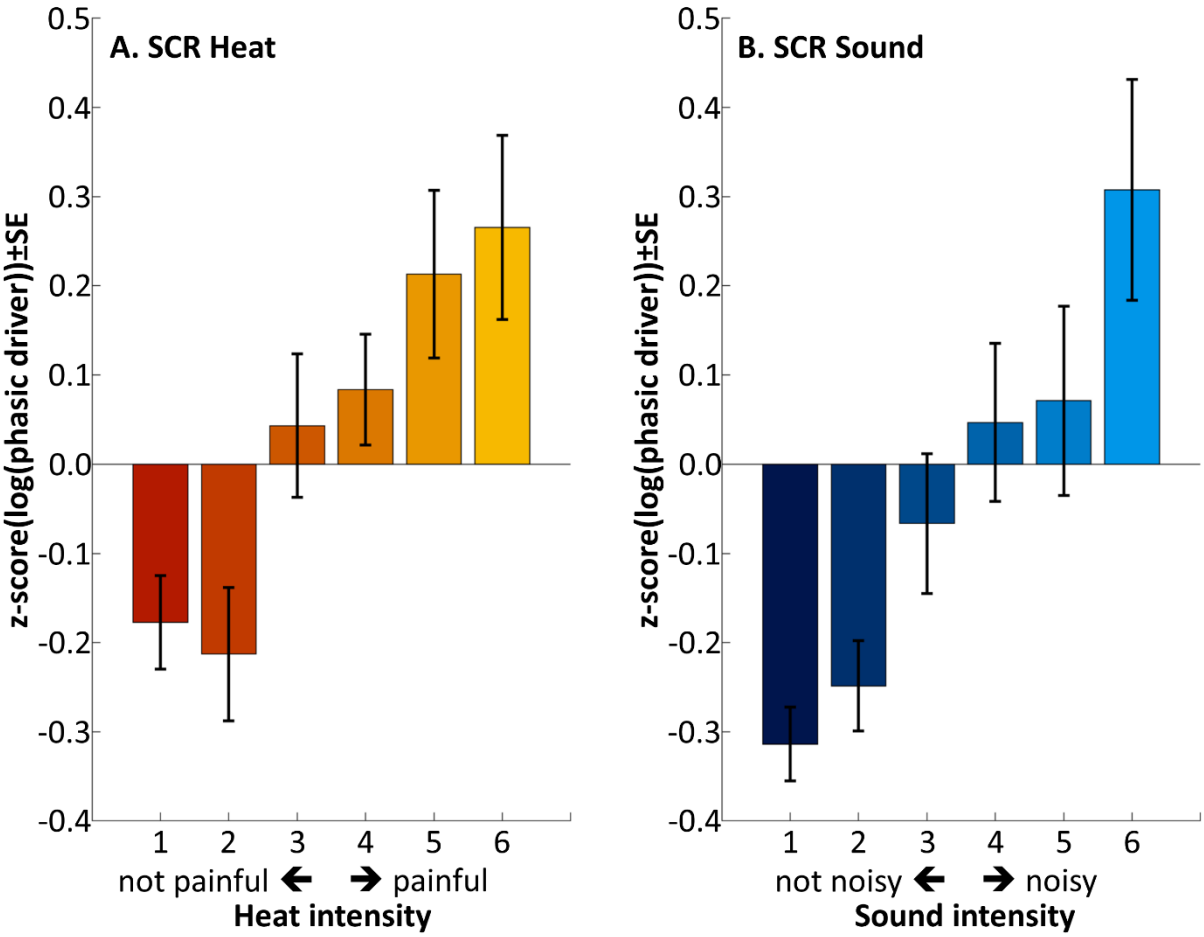


124

125 **Figure 2.** Skin conductance responses following heat (A) and sound stimuli (B). The pain and unpleasantness
126 thresholds were located between intensities 3 and 4, as per calibration.

bioRxiv preprint doi: https://doi.org/10.1101/581504; this version posted March 18, 2019. The copyright holder for this preprint (which was not certified by peer review) is the author/funder, who has granted bioRxiv a license to display the preprint in perpetuity. It is made available under aCC-BY 4.0 International license.

127 *Stimulus calibration results*

128 Mean heat pain threshold was at 43.5±1.1°C (range 40.5 to 45.4) and corresponded to 50 points on a
129 0 to 100 point visual analogue scale (VAS). Temperatures for stimulus intensities below and above
130 pain threshold, corresponding to VAS targets of 25, 35, 45, 55, 65 and 75, were 41.8±1.5°C,
131 42.5±1.3°C, 43.2±1.1°C, 43.9±1.0°C, 44.6±1.0°C and 45.3±1.1°C, respectively. Mean unpleasantness
132 threshold was at 83.0±6.7dBA (range 69.0-99.8). For additional details on heat and sound calibration,
133 see Methods, and S2 Table.

134

135 *Behavioral results*

136 The analysis of subjective ratings of sound and heat stimuli revealed a significant effect of modality
137 (t(320)=7.820, p=8e-14; average sound rated estimate±SE 13.3±1.7 VAS points higher than average
138 heat) (random intercept model; Figure 3) and a main effect of intensity (t(320)=42.014, p=2e-16;
139 11.8±0.3 VAS points per intensity step). The interaction between intensity and modality was also
140 significant (t(320)=-4.1529, p=4e-5; 2.3±0.6 VAS points shallower slope in sound, per intensity step).

141

bioRxiv preprint doi: https://doi.org/10.1101/581504; this version posted March 18, 2019. The copyright holder for this preprint (which was not certified by peer review) is the author/funder, who has granted bioRxiv a license to display the preprint in perpetuity. It is made available under aCC-BY 4.0 International license.

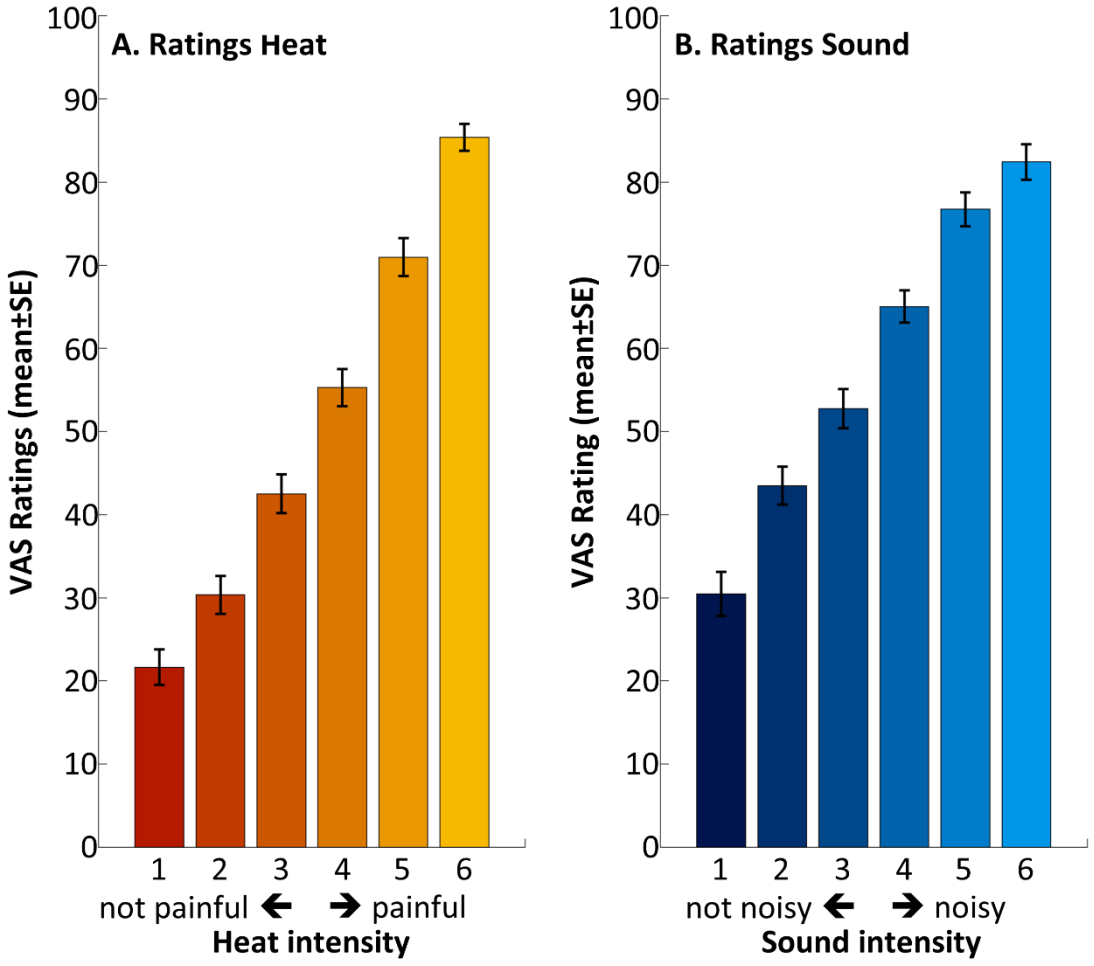


**Figure 3.** Behavioral ratings following heat (A) and sound stimuli (B). The pain and unpleasantness thresholds were located between intensities 3 and 4, as per calibration.

*Imaging results*

For either modality, a mask was used that was obtained from main effect activations a) larger than the respective comparator modality and b) larger than baseline (S1A Figure; see Methods for details). The same mask was applied to all contrasts reported in the following, with the exception of conjunction analyses, which were performed without mask. Application of the masks constrains the analyses to areas consistently activated during the respective modality.

bioRxiv preprint doi: https://doi.org/10.1101/581504; this version posted March 18, 2019. The copyright holder for this preprint (which was not certified by peer review) is the author/funder, who has granted bioRxiv a license to display the preprint in perpetuity. It is made available under aCC-BY 4.0 International license.

## Main effects of modality

To test for intermodal differences, we contrasted the main effects for heat and sound (Figure 4).

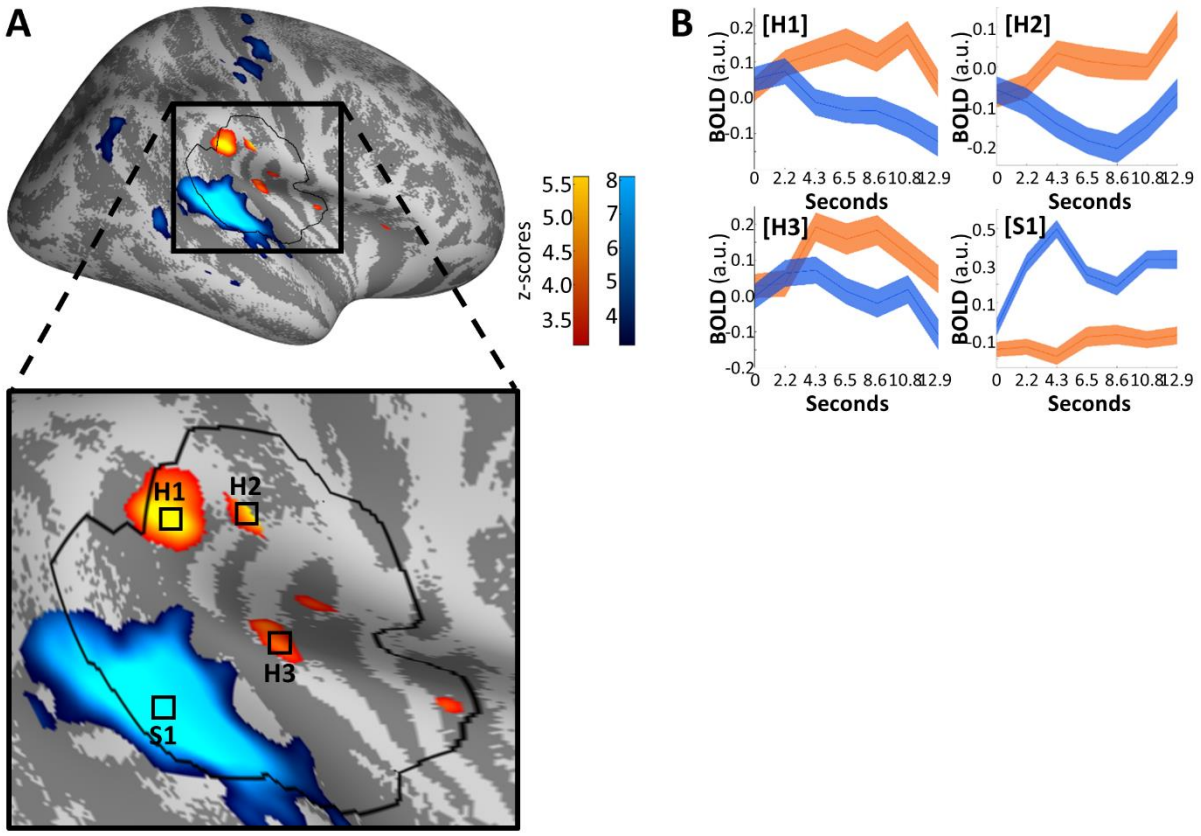


**Figure 4.** Differential effects of heat (orange) and sound (blue). Significant differences were found in the parietal operculum (H1, H2) and dorsal posterior insula (H3) for heat; in the superior temporal gyrus (S1) and Heschl's gyri for sound. **A.** Activations are thresholded at p(uncorrected)<0.001 and overlaid on an average brain surface for display purposes. The black line delineates the region of interest used for correction for multiple comparisons. See S2 Figure for peak locations in brain volume slices. **B.** Poststimulus plots of fMRI activation over all stimulus intensities (mean±SE). Subplots H1 through H3 show that heat-related activation (orange) dominates in the analyzed time frames (seconds 2.2 through 10.8, see Methods), while subplot S1 shows increased sound activation (blue).

The parietal operculum (secondary somatosensory cortex; peak MNI coordinates x=51, y=-30, z=28, Z=5.62, p(corrected)=1e-05; second peak at x=59, y=-23, z=25, Z=5.221, p(corrected)=1e-04) and

bioRxiv preprint doi: https://doi.org/10.1101/581504; this version posted March 18, 2019. The copyright holder for this preprint (which was not certified by peer review) is the author/funder, who has granted bioRxiv a license to display the preprint in perpetuity. It is made available under aCC-BY 4.0 International license.

dorsal posterior insula (x=40, y=-21, z=19, Z=4.175, p(corrected)=0.012) showed stronger activation for heat as compared to sound. Conversely, Heschl's gyri (primary auditory cortex; x=64, y=-24, z=7, Z=Inf, p(corrected)=4e-16) showed stronger activation for sound stimuli.

Of note, areas activated by either modality show no overlap, as determined via conjunction analyses, even at a liberal threshold of p(uncorrected)<0.001, of contrasts of heat or sound larger than baseline activation. The conjunction analysis did not use any masking; regardless, it did not yield significant results.

**Parametric modulation by stimulus intensity**

Irrespective of modality, main effects can be confounded by unspecific effects associated with the generic occurrence of an external stimulus, such as orientation and response preparation. Therefore, we performed an analysis investigating stimulus response functions (SRFs), i.e., testing for stronger BOLD responses for higher stimulus intensities.

We contrasted both modalities to identify areas with diverging SRFs within those areas showing a main effect of either modality, as determined above. For heat, we identified activity in the parietal operculum (x=57, y=-30, z=31, Z=3.999, p(corrected)=0.026) whose SRF diverges from that of the sound modality (Figure 5A). For sound, no significant activity prevailed, that is, no relationship of intensity and brain activity was found within the region of interest. Closer inspection of the time-course of the SRF in the heat modality (Figure 5B) indicates that the SRF's maximum slope coincides with the peak of the main effect, that is, the modulation of the main effect by intensity is strongest when the main effect itself is strongest.

bioRxiv preprint doi: https://doi.org/10.1101/581504; this version posted March 18, 2019. The copyright holder for this preprint (which was not certified by peer review) is the author/funder, who has granted bioRxiv a license to display the preprint in perpetuity. It is made available under aCC-BY 4.0 International license.

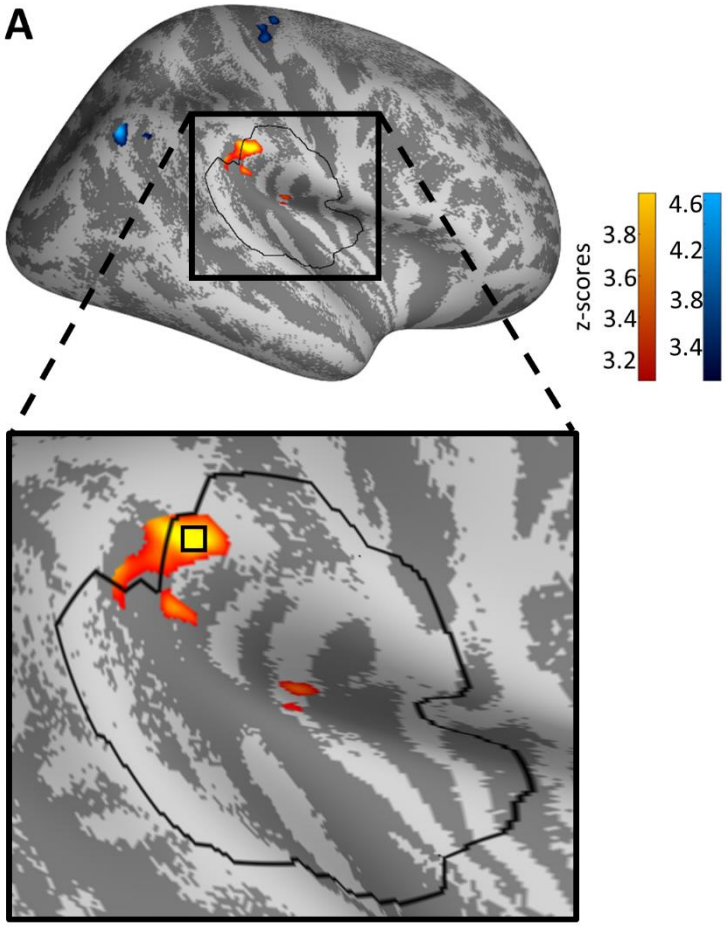


190

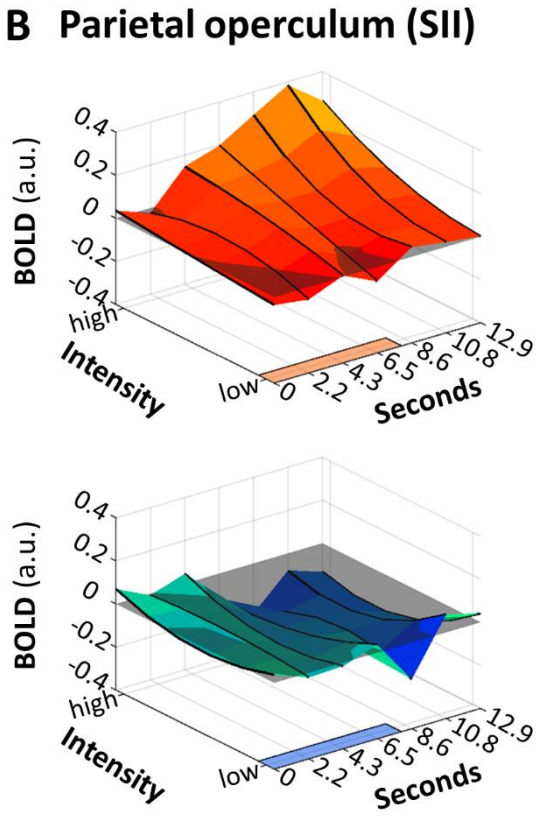


191

bioRxiv preprint doi: https://doi.org/10.1101/581504; this version posted March 18, 2019. The copyright holder for this preprint (which was not certified by peer review) is the author/funder, who has granted bioRxiv a license to display the preprint in perpetuity. It is made available under aCC-BY 4.0 International license.

**Figure 5.** Differential modulation by stimulus intensity for heat (orange) and sound (blue). Significant differences were found in the parietal operculum (H1) for heat. **A.** Activations are thresholded at p(uncorrected)<0.001 and overlaid on an average brain surface for display purposes. The black line delineates the region of interest used for correction for multiple comparisons. See S3 Figure for peak positions in brain volume slices, and S3B for sound activation in S1. **B.** Poststimulus plots of fMRI activation in vertex H1 during heat (orange) and sound (blue). The colored patches at the right axes show the stimulus duration. The lower left (y-)axes show the parametric modulation affecting the main effect (average size of the effect along the lower right (x-)axes): A straight line parallel to the y-axis indicates no change of the BOLD response depending on stimulus intensity, whereas the a sloped main effect along the y-axis indicates parametric modulation. In this area, the main effect of heat is mostly positively modulated by stimulus intensity, that is, higher stimulus intensities induce a higher extent of BOLD. The highest main effect activation occurs around second 10.8 (corresponding to scan 6), coinciding with the steepest slope of parametric modulation by intensity (y-axis).

Again, an unmasked conjunction analysis at a liberal threshold yielded no significant overlap of both modalities, when comparing contrasts with an SRF slope larger than zero for either modality.

**Parametric modulation by ratings**

Although relevant, physical stimulus intensity might not be directly mapped to neuronal activity, as a sensory signal undergoes multiple levels of processing before it reaches cortical areas. We therefore performed an additional analysis, where we investigated whether areas show BOLD responses that are correlated with subjects' behavioral ratings.

This analysis revealed that activity in the parietal operculum (x=55, y=-37, z=26, Z=5.091, p(corrected)=2e-04; x=58, y=-14, z=18, Z=4.312, p(corrected)=0.008) and the dorsal anterior insula (x=36, y=0, z=14, Z=4.276, p(corrected)=0.009; x=41, y=1, z=14, Z=3.849, p(corrected)=0.047) (Figure 6) showed a positive relationship to perceived intensity. This agrees with and extends results from the previous analysis in which BOLD responses were correlated with stimulus intensity in the parietal

bioRxiv preprint doi: https://doi.org/10.1101/581504; this version posted March 18, 2019. The copyright holder for this preprint (which was not certified by peer review) is the author/funder, who has granted bioRxiv a license to display the preprint in perpetuity. It is made available under aCC-BY 4.0 International license.

218 operculum. For sound, no significant activity prevailed, that is, no relationship of ratings and brain

219 activity was found.

220

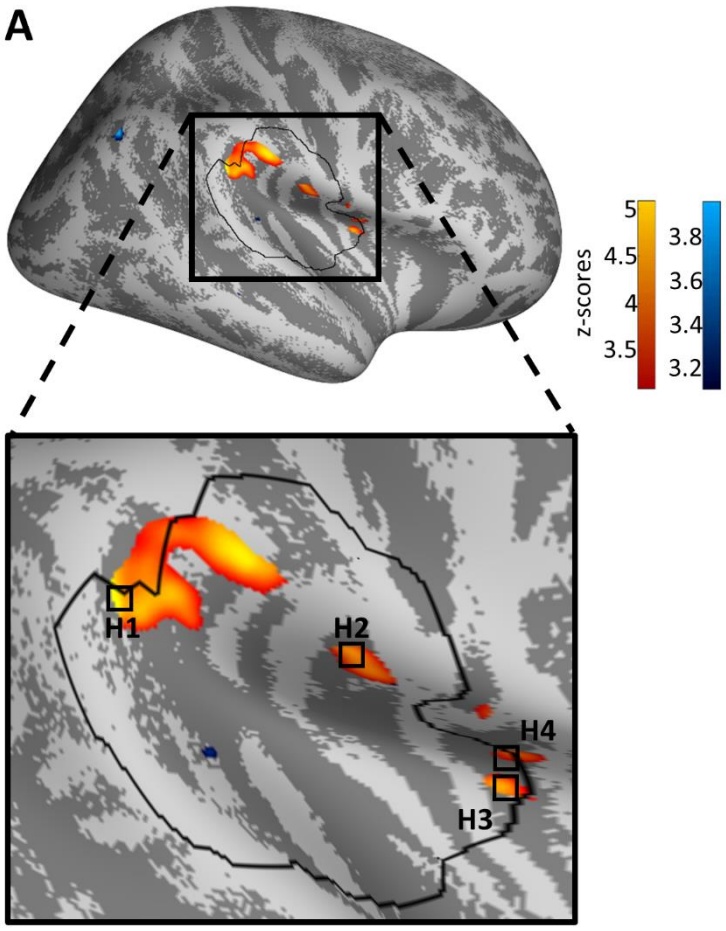


221

222

bioRxiv preprint doi: https://doi.org/10.1101/581504; this version posted March 18, 2019. The copyright holder for this preprint (which was not certified by peer review) is the author/funder, who has granted bioRxiv a license to display the preprint in perpetuity. It is made available under aCC-BY 4.0 International license.

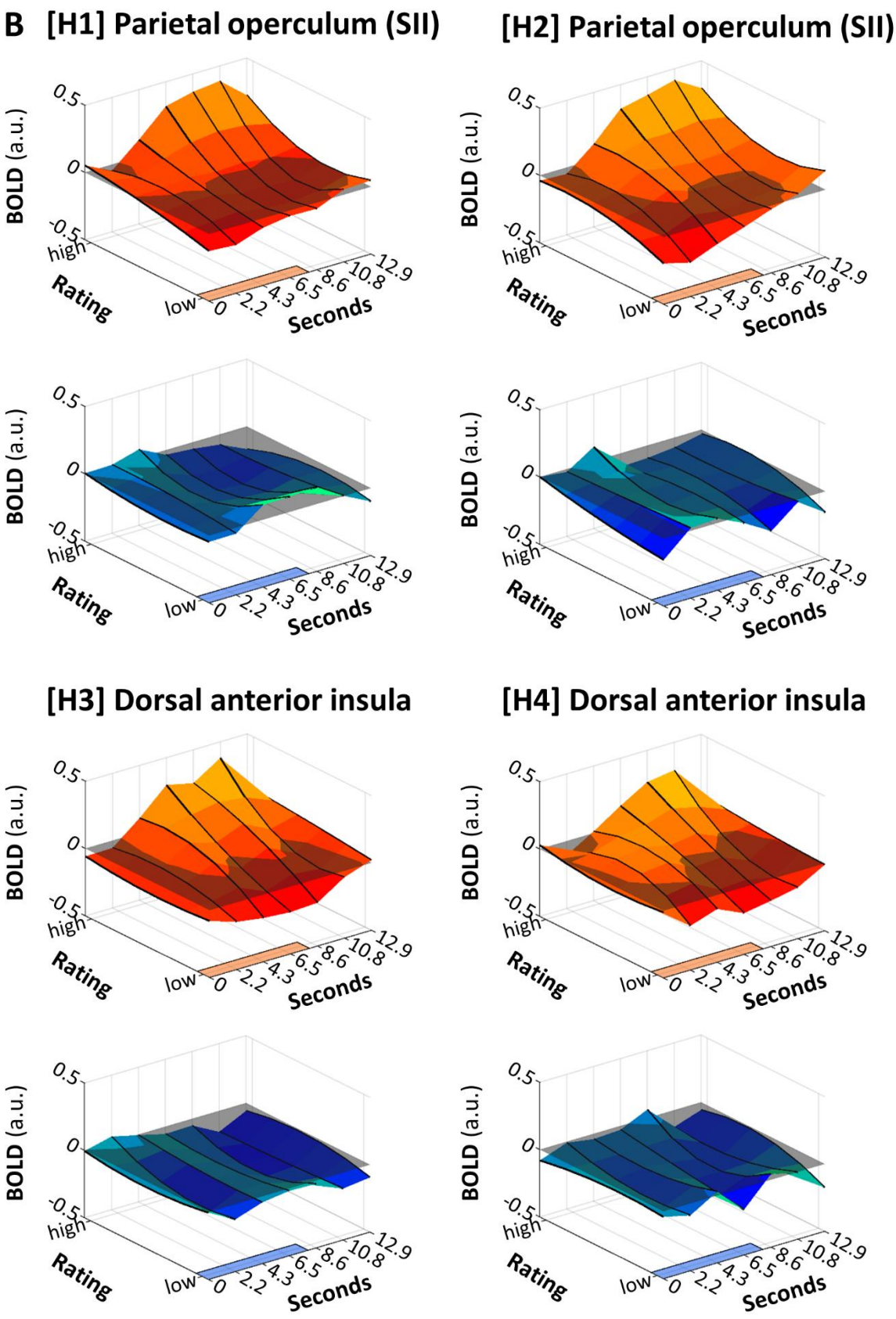


**Figure 6.** Differential modulation by ratings for heat (orange). Significant differences were found in the parietal operculum (H1, H2), central operculum (H3) and dorsal anterior insula (H4). **A.** Activations are thresholded at

bioRxiv preprint doi: https://doi.org/10.1101/581504; this version posted March 18, 2019. The copyright holder for this preprint (which was not certified by peer review) is the author/funder, who has granted bioRxiv a license to display the preprint in perpetuity. It is made available under aCC-BY 4.0 International license.

p(uncorrected)<0.001 and overlaid on an average brain surface for display purposes. The black line delineates the region of interest used for correction for multiple comparisons. See S4 Figure for peak positions in brain volume slices. **B.** Poststimulus plots of fMRI activation in vertices H1 through H4 during heat (orange) and sound (blue). The colored patches at the right axes show the stimulus duration. The lower left (y-)axes show the parametric modulation by ratings that are affecting the main effect.

As before, in the unmasked conjunction analysis of contrasts where rating correlated with the BOLD responses, no regions with significant overlap were found.

**Imaging results distinguishing stimuli perceived below and above thresholds**

So far, all analyses pooled over non-painful and painful heat percepts. To further investigate pain-related responses, we separated those stimuli reported as non-painful from those reported as painful (i.e., subthreshold versus suprathreshold), and similarly for unpleasant versus non-unpleasant sounds. We followed an axiomatic approach to identify areas where activity under painful stimulation could neither be explained by an overlap with activity under non-painful heat (as would be the case, e.g., in thermosensitive areas), or by an overlap with activity following unpleasant sound (e.g., in areas processing stimulus salience). In particular, we posited that a region can be characterized as preferentially pain-processing if the following conditions hold:

- Axiom 1: The effect of suprathreshold – i.e., painful – stimulation should be larger than that of subthreshold – i.e., heat – stimulation.
- Axiom 2: The effect of suprathreshold heat stimulation should be larger than that of suprathreshold sound stimulation.
- Axiom 3: The relationship of ratings and BOLD – i.e., the slope of the stimulus response function – should be stronger for suprathreshold heat than for subthreshold heat.

bioRxiv preprint doi: https://doi.org/10.1101/581504; this version posted March 18, 2019. The copyright holder for this preprint (which was not certified by peer review) is the author/funder, who has granted bioRxiv a license to display the preprint in perpetuity. It is made available under aCC-BY 4.0 International license.

- Axiom 4: The relationship of ratings and BOLD should be stronger for suprathreshold heat than for suprathreshold sound.

Each of the axioms was evaluated at a significance threshold of p=0.05, corrected for family-wise error. After joint application of each axiom, analysis revealed activation in the posterior parietal operculum (x=56, y=-37, z=25, Z=5.519, p(corrected)=0.035) (Figure 7), adjacent to the supramarginal gyrus.

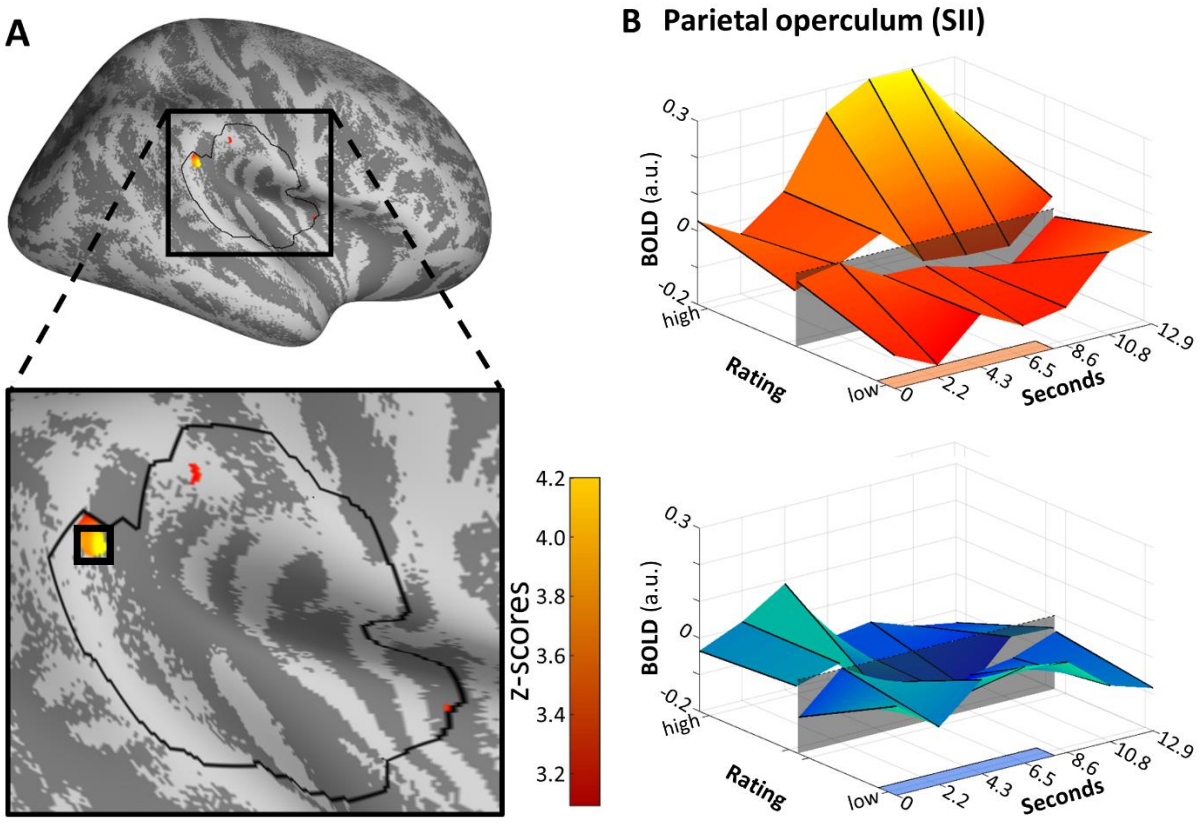


**Figure 7.** Areas that fulfill the axiomatic requirements of differential activation during pain compared to heat and sound. In detail, these axioms were 1) a larger effect of suprathreshold heat compared to subthreshold heat, 2) a larger effect of suprathreshold heat compared to suprathreshold sound, 3) a stronger relationship of BOLD with pain ratings than with heat ratings, 4) a stronger relationship of BOLD with pain ratings than with unpleasantness ratings. Significant activation was found in the parietal operculum (H1). **A.** Activations are thresholded at p(uncorrected)<0.001 and overlaid on an average brain surface. The black line delineates the SVC mask. See S5 Figure for peak positions in brain volume slices. **B.** Poststimulus plots of fMRI activation in

bioRxiv preprint doi: https://doi.org/10.1101/581504; this version posted March 18, 2019. The copyright holder for this preprint (which was not certified by peer review) is the author/funder, who has granted bioRxiv a license to display the preprint in perpetuity. It is made available under aCC-BY 4.0 International license.

vertex H1 during heat (orange) and sound (blue). The shaded patch in the center signifies the pain threshold (for heat) and unpleasantness threshold (for sound). The colored patches at the right axes show the stimulus duration.

## Discussion

This study aimed to identify regions relevant for heat pain processing, and to determine whether their activation can be explained by salience. We used individually calibrated, parametrically graded heat stimuli, and an auditory control condition. Heat and sound stimuli were matched for arousal as indicated by similar skin conductance responses. Furthermore, we employed surface-based analyses to mitigate spatial inaccuracies of 3D smoothing.

Main effects for heat were identified in the parietal operculum and the posterior insula, main effects of acoustic stimuli were observed in the superior temporal gyrus. More importantly, in the parietal operculum, we observed a differential correlation of brain activity with ratings above versus below the heat pain threshold, concurrent with a differential correlation with ratings under painful heat versus unpleasant sound. As we have matched both modalities for salience, these results unequivocally rule out that activity in this area is simply related to stimulus salience, and suggests a more dedicated role in heat pain processing.

Using SCR as an autonomic readout of arousal [15,20,21] allowed us to establish comparable salience of the stimulus material, independent of any behavioral assessments. Although salience can be assessed psychometrically [5] and research exists to establish concurrent validity of salience ratings within individual modalities [22], to our knowledge, such ratings have not been validated cross-modally. It is likely that salience ratings are scaled differently according to some modality-specific perceptual range. Our results support this notion, as we have observed a prevailing difference in behavioral ratings between the two modalities (sound was, on average, rated as more aversive, but

bioRxiv preprint doi: https://doi.org/10.1101/581504; this version posted March 18, 2019. The copyright holder for this preprint (which was not certified by peer review) is the author/funder, who has granted bioRxiv a license to display the preprint in perpetuity. It is made available under aCC-BY 4.0 International license.

had a shallower slope with increasing intensities). This means that a reliance on behavioral ratings alone could compound SCR dissimilarities between comparator modalities.

With six graded stimulus intensities per modality, our design allowed for the assessment of stimulus response functions as opposed to simple mean comparisons between a single intensity and a low-level baseline, or between single sub- and suprathreshold stimuli. Apart from physical intensities, this also allowed us to use a large range of individual ratings as predictors. Using these perceived intensities, we were able to directly investigate competing modes of encoding. For example, a brain area may encode heat intensity, regardless of pain, or it may be inactive below threshold but encode pain intensity above threshold [12,13,23]. In the analysis distinguishing between sub- and suprathreshold stimuli, we see a clear pain-intensity-related response in the parietal operculum (Figure 7). While not a main focus of this paper, we do see a shift in SRFs even within small cortical distances: For example, an area rostral (x=55, y=-26, z=26) to the more heat pain-dedicated posterior parietal operculum (x=56, y=-37, z=25) fails to register differences in the parametric modulation by sub- and suprathreshold heat (Figure 8).

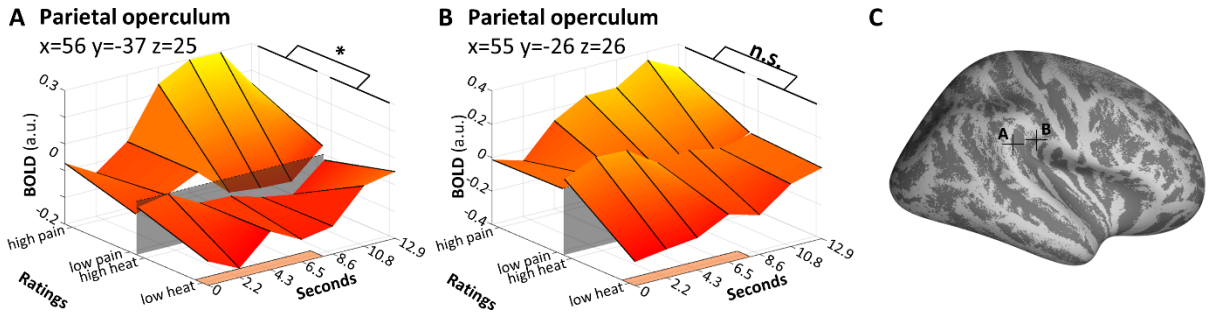


**Figure 8.** Distinction of areas with stimulus response functions corresponding to the axioms, or not (heat modality only). A. The slopes of subthreshold (heat) versus suprathreshold (pain) activation as described in Figure 7. Heat slopes are shallower than pain slopes. B. Slopes of heat and pain activation in an opercular vertex slightly anterior to A, as determined per conjunction of heat and pain parametric modulation. Slopes are more aligned, preventing the contrasted activation (pain>heat) of reaching significance. Note that this is not a

bioRxiv preprint doi: https://doi.org/10.1101/581504; this version posted March 18, 2019. The copyright holder for this preprint (which was not certified by peer review) is the author/funder, who has granted bioRxiv a license to display the preprint in perpetuity. It is made available under aCC-BY 4.0 International license.

311 formal comparison to A. **C.** Location of the vertices described in A and B. B is in an adjacent area about 1 cm
312 surface distance rostral from A.

313

314 Areas in the insula and surrounding cortical areas are characterized by extreme cortical folding. We
315 therefore implemented a subject specific surface-based fMRI analysis. This prevents contamination
316 of gray matter voxels by signal from white matter and cerebrospinal fluid. Furthermore, surface-
317 based analyses circumvent potential issues arising from three-dimensional smoothing which
318 accidently mixes signals from structures adjacent in three-dimensional space which are actually
319 distant from each other. For example, the parietal operculum is directly adjacent to the superior
320 temporal gyrus in three-dimensional space, but their neurons are separated by the entire insular
321 fold. Smoothing with a three-dimensional kernel therefore includes activity across the lateral sulcus
322 (alongside noise from white matter and corticospinal fluid), thereby increasing error terms and
323 decreasing sensitivity of the respective comparisons. Importantly, in this case, three-dimensional
324 smoothing could also generate erroneous overlaps between conditions. Surface-based analyses have
325 been found to increase sensitivity and reduce deviations when normalizing from native to standard
326 space [24].

327 In contrast to previous multimodal studies, we explicitly chose modalities where the aversiveness
328 would be generated by virtue of physical intensity. This is naturally the case with painful stimulation,
329 but several studies did not use aversive stimulation in non-painful control modalities (for example
330 [9], who used low-intensity tactile stimulation). Consequently, the acoustic modality was chosen
331 because stimuli can be generated in close analogy to heat, by altering the physical intensity of the
332 stimuli.

333 For our analyses of neuronal activity, we have focused on the posterior insula and adjacent areas.
334 The insula is of particular interest, because its involvement in pain has been well-documented
335 [4,9,25]. Furthermore, it has been hypothesized to perform polymodal magnitude estimation [23,26],

bioRxiv preprint doi: https://doi.org/10.1101/581504; this version posted March 18, 2019. The copyright holder for this preprint (which was not certified by peer review) is the author/funder, who has granted bioRxiv a license to display the preprint in perpetuity. It is made available under aCC-BY 4.0 International license.

and is also involved in salience processes [27,28]. Unambiguous data concerning the involvement of the insular cortex in pain processing also comes from direct cortical stimulation studies [29–31]. Consequently, it is a prime candidate to assess overlaps and differences in activation patterns.

With its reliable activation following painful stimulation, we can unequivocally establish the parietal operculum as an important area of heat pain processing, whose activity cannot be explained by stimulus salience. The area not only shows increased activation when comparing pain and other modalities (heat, sound), but also exhibits a monotonic increase with perceived pain. The peak of the BOLD response following pain clearly coincides with the largest modulation by behavioral ratings of pain, roughly 8 seconds after stimulus onset (Figure 7B). Importantly, this area has close functional connections with the posterior insula [32], another area of interest [9,16].

Interestingly, we were not able to replicate earlier findings [5,33] of substantial overlap of activation regardless of modality, even at a lower threshold. This might be related to the differences in stimulus parameters between the studies: Previous multisensory studies have used rapid onset stimuli of very short duration, whereas ours were considerably longer (8 seconds plateau, circa 9.5 seconds with upward/downward slopes). It is possible that with increasing brevity and suddenness of the stimuli, the extent of unspecific orientation responses and other attention related processes is disproportionally larger, and therefore a larger overlap of neuronal activation can be observed [34]. If true, this overlap would naturally be determined, to a large extent, by unspecific and not pain-related activations such as salience.

Brain responses evoked by stimuli in different sensory modalities might follow different time courses; systematic differences may, for example, arise from different conduction speeds of fibers relaying auditory (mostly very fast Aα fibers), thermoceptive (mostly slow C fibers) and nociceptive input (Aδ and C fibers), compounded by the fact that thermal stimulation (in this setup) occurs at a distal site compared to auditory stimulation. Therefore, in analogy to [5], we opted for analyzing the time-course of all imaging data by using finite impulse responses as basis functions. This largely avoids the

bioRxiv preprint doi: https://doi.org/10.1101/581504; this version posted March 18, 2019. The copyright holder for this preprint (which was not certified by peer review) is the author/funder, who has granted bioRxiv a license to display the preprint in perpetuity. It is made available under aCC-BY 4.0 International license.

361 constraints and biases implicit in comparing mean activations obtained by pre-defined hemodynamic
362 response functions.

363 Some limitations apply to the present research.

364 The study used stimuli of mild to moderate aversiveness (calibrated to a maximum of 50 if rescaled
365 to a conventional, 0-100 suprathreshold visual analogue scale). This aspect, too, could be amended
366 to cover a broader range, albeit increasing the risk of carry-over effects such as sensitization,
367 particularly with longer stimulus duration. Additionally, the use of only a single trial-based, post-
368 stimulus rating of stimulus intensity could be criticized. In fact, one common recommendation for
369 pain measurement is to distinguish multiple pain dimensions [1], most frequently intensity and
370 unpleasantness [35], although these aspects tend to be highly correlated in non-interventional
371 designs [36,37]. Given the SCR-based approach to equalize salience and to include more stimulus
372 repetitions, we opted against multiple VAS for protocol reasons, namely ease of measurement and to
373 avoid confusion.

374 While we have identified areas preferentially active in painful heat as compared to unpleasant
375 sound, we cannot claim that these areas are specific for pain. In fact, it is important to note that
376 specificity cannot be ascertained with a limited number of control conditions [10,38]. We concur that
377 the notion of specificity is more academic in nature than might benefit the field [3]. The preferences
378 of certain areas to process various inputs – whether visual, acoustic, nociceptive – is best construed
379 as a matter of degree, that is, a question of specialization rather than specificity, as has been
380 suggested for functions unrelated to pain [39]. Nevertheless, the rigorous axiomatic approach allows
381 for a strong hypothesis ascribing the parietal operculum a dedicated role in pain processing.

382

bioRxiv preprint doi: https://doi.org/10.1101/581504; this version posted March 18, 2019. The copyright holder for this preprint (which was not certified by peer review) is the author/funder, who has granted bioRxiv a license to display the preprint in perpetuity. It is made available under aCC-BY 4.0 International license.

## Materials and Methods

The protocol was approved by the local Ethics Committee (Ethikkommission der Ärztekammer Hamburg, vote PV4745) and conformed to the standards laid out by the World Medical Association in the Declaration of Helsinki. Participants gave written informed consent prior to participation.

*Exclusion criteria*

A list of exclusion criteria is provided in Table 1.

**Table 1.** Exclusion criteria.

- Age younger than 18, older than 40
- Sufficient visual acuity, correction with contact lenses only
- Conditions disqualifying for MR-scanners (e.g. claustrophobia, wearing a pacemaker)
- Ongoing participation in pharmacological studies, or regular medication intake (e.g. analgesics)
- Analgesics use 24h prior to the experiment
- Pregnancy or breastfeeding
- Chronic pain condition
- Manifest depression (as per Beck Depression Inventory II, BDI-II, cutoff 14 as per [40])
- Somatic symptom disorder (as per Patient Health Questionnaire, PHQ15, cutoff 10 as per [41])
- Other neurological, psychiatric or dermatological conditions
- Inner ear conditions
- Head circumference >60 cm (for second cohort, due to device constraints)

bioRxiv preprint doi: https://doi.org/10.1101/581504; this version posted March 18, 2019. The copyright holder for this preprint (which was not certified by peer review) is the author/funder, who has granted bioRxiv a license to display the preprint in perpetuity. It is made available under aCC-BY 4.0 International license.

393 *Psychophysiological recordings*

394 Electrodermal activity was measured with MRI-compatible electrodes on the thenar and hypothenar
395 of the left hand. Electrodes were connected to Lead108 carbon leads (BIOPAC Systems, Goleta, CA,
396 USA). The signal was amplified with an MP150 analog amplifier (also BIOPAC Systems). It was
397 sampled at 1000 Hz using a CED 1401 analog-digital converter (Cambridge Electronic Design,
398 Cambridge, UK) and downsampled to 100 Hz for analysis.

399 Analysis was performed using the Ledalab toolbox for MATLAB [42]. Single subject data were
400 screened for artifacts which were removed if possible by using built-in artifact correction algorithms.
401 Using a deconvolution procedure, we computed phasic skin conductance (SCR). SCR occurring after
402 stimulus onset and within stimulus duration was used for measuring autonomic arousal as a proxy
403 for stimulus salience. Response windows were defined by visual inspection, per modality: between
404 2.0 s and 4.5 s for heat, and between 1.5 s and 4.0 s for sound. Results were log- and z-transformed
405 to reduce the impact of intra- and interindividual outliers [15]. Subsequently, SCR was averaged
406 within subjects for two modalities (heat/sound) and six stimulus intensities each, yielding twelve
407 values per person.

408 SCR was used because it is an objective measure of general sympathetic activity, and therefore a
409 measure of arousal and stimulus salience [15,20,21] which is routinely used in assessing painful
410 [14,43,44] as well as acoustic stimulation [45].

411

412 *fMRI acquisition and preprocessing*

413 Functional and anatomical imaging was performed using a TRIO 3T MR Scanner (Siemens, Erlangen,
414 Germany) with a 12-channel head coil. An fMRI sequence of 36 transversal slices of 2 mm thickness
415 was acquired using T2*-weighted gradient echo-planar imaging (EPI; 2150 ms TR, 25 ms TE, 80° flip
416 angle, 2x2x2 mm voxel size, 1 mm gap, 216x216x107 mm field of view, acceleration factor of 2 with
417 generalized autocalibrating partially parallel acquisitions reconstruction, GRAPPA). Coverage did not

bioRxiv preprint doi: https://doi.org/10.1101/581504; this version posted March 18, 2019. The copyright holder for this preprint (which was not certified by peer review) is the author/funder, who has granted bioRxiv a license to display the preprint in perpetuity. It is made available under aCC-BY 4.0 International license.

include the apical parts of the frontal/parietal lobes. Additionally, a T1-weighted MPRAGE anatomical image was obtained for the entire head (voxel size 1x1x1 mm, 240 slices).

For each subject, fMRI volumes were realigned to the mean image in a two-pass procedure, and co-registered to the anatomical image using affine transformations. Anatomical images were segmented into tissue types, and individual brain surfaces generated, using the CAT12 toolbox for SPM (Christian Gaser & Robert Dahnke, http://www.neuro.uni-jena.de/cat/).

*Analysis of imaging data*

Subject-level analyses were performed on the 3D (volume) data in native space without smoothing, using an implicit mask at 0.6 to facilitate subsequent (surface) processing. We computed general linear models to identify brain structures involved in the processing of each stimulus modality, as well as the encoding of intensities within those modalities (volume data not shown). All analyses were performed with seventh order FIR basis functions, of which bins 2 to 6 are considered when comparing conditions. This amounts to seconds 4.3 through 12.9 post stimulus onset. Realignment (motion) parameters as well as regressors obtained from ventricular motion were included as nuisance variables, to mitigate motion-related artifacts.

We first set up a model including one regressor for stimulus main effects in each modality. Another two regressors – one linear, one quadratic – encoding stimulus intensities 1 through 6 were added per modality, as parametric modulators. The second model likewise included main effects, and behavioral ratings as linear and quadratic parametric modulators. Finally, the third model further distinguished the two modalities in stimuli perceived as below and above the respective thresholds (pain for heat stimuli, unpleasantness for sound stimuli), yielding four main effect regressors (subthreshold heat, suprathreshold heat – i.e., pain –, subthreshold sound, suprathreshold sound). Behavioral ratings were again included as linear parametric modulators; quadratic modulation was not considered to preclude overfitting.

bioRxiv preprint doi: https://doi.org/10.1101/581504; this version posted March 18, 2019. The copyright holder for this preprint (which was not certified by peer review) is the author/funder, who has granted bioRxiv a license to display the preprint in perpetuity. It is made available under aCC-BY 4.0 International license.

Results from subject-level analyses were mapped to brain surfaces obtained via the CAT12 segmentation procedure. The mapped subject-level results were then resampled to correspond to surface cortical templates, and smoothed with a 6 mm full width-half maximum 2D kernel. Group-level analyses were performed including the mapped contrasts, which are described in the Results section.

Masking was used to distinguish either modality, as the ANOVAs employed are unsigned and in principle detect differences in activation regardless of direction. Therefore, we obtained signed (that is, unconstrained by p values) masks from calculating a conjunction from significant voxels of a) a t-test contrasting the average main effects of either modality (i.e., where activation following heat was larger than that following sound, and vice versa), and b) a t-test contrasting either modality to low-level baseline (i.e., where activation following heat – or sound, respectively – was larger than zero. This yielded a single mask for both modalities, which was applied to all analyses (unless otherwise noted) (S1B Figure).

For the purpose of this study, we focused on the hemisphere contralateral to the stimulation, in our case the right hemisphere. In general, the larger part of activity following pain is contralateral to the stimulation site, but is known to be bilateral in several key areas such as the secondary somatosensory cortex and the insula [46].

Furthermore, we focused on the insula and directly adjacent areas for small volume correction of significance level. In particular, we included the granular insular cortex (Ig1, Ig2) as well as the parietal operculum (OP1, OP2) and primary auditory cortex (Te1.1), using the SPM Anatomy Toolbox (version 2.2b [47]). This mask was mapped to a template brain surface, then smoothed with a 4 mm 2D kernel to close gaps. The resulting binary mask (S1A Figure) was roughly centered around previously reported coordinates (x=[-]34, y=-20, z=18) involving areas putatively dedicated to pain processing [9]. It was used for small volume correction of second level analyses, where results were considered after correction for family-wise error rate of $p<0.05$.

bioRxiv preprint doi: https://doi.org/10.1101/581504; this version posted March 18, 2019. The copyright holder for this preprint (which was not certified by peer review) is the author/funder, who has granted bioRxiv a license to display the preprint in perpetuity. It is made available under aCC-BY 4.0 International license.

468 *Psychometry*

469 Owing to the study's aim to compare two stimulus modalities (heat and sound), they had to be
470 presented and rated in an analogous fashion. Therefore, while retaining the intuitive descriptor
471 "painfulness" for rating noxious heat (as composite measure of intensity and unpleasantness), we
472 settled on "unpleasantness" as descriptor for sounds. This also seemed warranted considering the
473 high correlation of intensity and unpleasantness measures in heat pain [37], while unpleasantness is
474 one of the definitional criteria of pain [2].

475 Furthermore, since we wanted to use graded stimuli both below and above the respective thresholds
476 (pain threshold for heat, unpleasantness threshold for sound), we deviated from the more common
477 simple visual analogue scales (VAS) and devised two partitioned 0 to 100 VAS for both modalities
478 (Figure 1A).

479 For heat, it captured both painful and non-painful sensations. Subjects were instructed to indicate
480 heat intensity in absence of pain in the 0 through 49 range, and heat pain intensity in the 50 through
481 100 range. Hence, anchors were displayed for "no sensation" (0), "minimal pain" (50), and
482 "unbearable pain" (100). Pain was operationalized as the presence of sensations other than pure
483 heat intensity, such as stinging or burning, as per the guidelines of the German Research Network on
484 Neuropathic Pain [48].

485 Likewise, for sound, both unpleasant and non-unpleasant sensations were captured by the VAS.
486 Subjects were instructed to indicate loudness in absence of unpleasantness in the 0 through 49
487 range, and loudness unpleasantness in the 50 through 100 range. Anchors were displayed for
488 "inaudible" (0), "minimally unpleasant" (50), and "extremely unpleasant" (100). Unpleasantness was
489 operationalized as a bothersome quality of the sound emerging at a certain loudness.

490

491

bioRxiv preprint doi: https://doi.org/10.1101/581504; this version posted March 18, 2019. The copyright holder for this preprint (which was not certified by peer review) is the author/funder, who has granted bioRxiv a license to display the preprint in perpetuity. It is made available under aCC-BY 4.0 International license.

492 *Heat stimuli and calibration*

493 Heat stimuli were delivered using a CHEPS thermode (Medoc, Ramat-Yishai, Israel). Stimulation sites
494 were located on the radial surface of the forearm. Three separate sites were used for calibration and
495 either experimental session, to avoid changes in heat/pain perception due to repeated stimulation.
496 Around the middle of the forearm (half distance between crook of the arm and distal wrist crease;
497 see Figure 1B), three stimulation sites were marked prior to the experimental sessions. For
498 calibration, a medial site on the distal part of the forearm was used; for experimental sessions 1 and
499 2, two adjacent proximal sites were used, in counterbalanced order. During both calibration
500 procedure and experimental sessions, baseline temperature was set to 35°C, and rise and fall rate
501 were set to 15°C per second. The duration of heat stimuli was set to eight seconds at target
502 temperature (plateau), except for preexposure stimuli whose plateau duration was zero (and thus
503 only consisted of temperature up- and downramping).

504 A two-step stimulus calibration was performed for each subject, to determine three temperatures
505 below the individual pain threshold, and three above. Calibration was performed with the MR-
506 scanner running the same sequence as during the actual experimental sessions, to mimic ambient
507 conditions [49]. fMRI data from calibration was later discarded.

508 In a first calibration step, the pain threshold was determined. Subjects were preexposed to four brief
509 heat stimuli. Preexposure started at 42°C and each consecutive stimulus was increased by 0.5°C, up
510 to 43.5°C. If a subject indicated the last stimulus as painful, starting temperature for the following
511 procedure was set to 43°C, else to 44°C. We then used a probabilistic tracking procedure for
512 threshold determination, assuming a normal distribution of pain perception around the actual
513 threshold [50]. Eight full-length stimuli were presented and received a binary rating (painful or not
514 painful). Depending on the rating of the previous stimulus, each consecutive stimulus was set to a
515 higher or lower temperature according to the probability informed by previous pivot points. The final
516 temperature was defined as threshold intensity.

bioRxiv preprint doi: https://doi.org/10.1101/581504; this version posted March 18, 2019. The copyright holder for this preprint (which was not certified by peer review) is the author/funder, who has granted bioRxiv a license to display the preprint in perpetuity. It is made available under aCC-BY 4.0 International license.

In a second calibration step, eight stimuli unevenly spaced around threshold intensity (from -2°C to +1.6°C, with smaller intervals towards ±0°C) were rated on the partitioned VAS described above. After the procedure, linear regression was used to calculate target temperatures H1 through H6, to obtain subthreshold VAS ratings of 25, 35 and 45 (H1–H3), and suprathreshold VAS ratings of 55, 65 and 75 (H4–H6).

These six intensities were used throughout the experimental sessions.

*Sound stimuli and calibration*

Sound stimuli were delivered using MR-compatible headphones (NordicNeuroLabs, Bergen, Norway). A pure sound (frequency 1000 Hz, sampling rate 22050 Hz) was generated using MATLAB. A log function was used to translate increases in (physical) amplitude to smooth gradual increases in (psychoacoustic) loudness, to mimic the heat stimuli's temperature ramps. Like the heat stimuli, sound stimuli were presented for eight seconds at target loudness (plateau), and the scanner was running a dummy EPI sequence throughout to mimic actual conditions [51].

A two-step stimulus calibration was performed for each subject, to determine three sounds below the individual unpleasantness threshold, and three above. The general procedure was analogous to the one used for heat.

In a first calibration step, the individual loudness unpleasantness threshold (in percent of maximum amplitude of ~100 dB, allowing for safe exposure even at maximum intensities [52]) was determined by an ascending methods of limits-procedure. Six sounds of gradually increasing loudness were played. The calibration sounds differed in the steepness of the loudness ramps, taking between 9 and 15 seconds to reach peak amplitude. Subjects were asked to indicate the point where the loudness became unpleasant. The mean of the last four of the six stimuli was defined as threshold loudness.

bioRxiv preprint doi: https://doi.org/10.1101/581504; this version posted March 18, 2019. The copyright holder for this preprint (which was not certified by peer review) is the author/funder, who has granted bioRxiv a license to display the preprint in perpetuity. It is made available under aCC-BY 4.0 International license.

In a second calibration step, 16 stimuli unevenly spaced around threshold loudness were presented (from -15% to +15%, smaller intervals towards ±0%), with stimulus characteristics set to mimic those of heat stimuli (roughly 0.75 s ramps up and down, plus 8 s plateau loudness). As with heat ratings, linear regression was used to calculate target amplitudes S1 through S6, namely to obtain subthreshold VAS ratings of 25, 35 and 45 (S1–S3), and suprathreshold VAS ratings of 55, 65 and 75 (S4–S6). For the second cohort, VAS targets were informed by the corresponding mean SCR amplitude of the first cohort (see "Differences between first and second cohort").

Finally, ramping characteristics of sound stimuli (the seconds it took to plateau) were set to correspond to those of the respective intensity's heat stimuli, such that corresponding intensities of both modalities had an identical overall length (ramps plus plateau).

*Stimulus presentation during experimental sessions*

After calibration, the thermode stimulation site was changed, and the first experimental session commenced. Heat and sound stimuli were presented in alternation, so that trials of the same modality were spaced with an intertrial interval of approximately 30 seconds. Each trial followed the same basic structure (Figure 1C).

Within each modality, the six intensities were pseudorandomized in microblocks. Randomization was performed such that each sequence of six stimuli contained one instance of each intensity. It was further constrained such that the very first stimulus was never chosen from the highest two intensities, and two consecutive intensities were never more than 3 intensity steps different (e.g., the intensity following heat intensity 1 could not exceed heat intensity 4).

After changing thermode stimulation site again, session 2 commenced with identical protocol (albeit different randomization).

bioRxiv preprint doi: https://doi.org/10.1101/581504; this version posted March 18, 2019. The copyright holder for this preprint (which was not certified by peer review) is the author/funder, who has granted bioRxiv a license to display the preprint in perpetuity. It is made available under aCC-BY 4.0 International license.

Visual cues and VAS rating scales were displayed in the scanner using back-projection via a 45° mirror placed atop the head coil.

*Selection of subsample for analysis with comparable SCR between modalities*

In total we assessed two cohorts of 32 subjects and 26 subjects. To obtain an "SCR-equalized" subsample from all subjects (N=58 with 2 sessions, that is a total of 116 experimental sessions), in a first step, we excluded all sessions where the correlation between ratings (that is, perceived stimulus intensity/unpleasantness) and SCR was lower than or equal to zero, so that only subjects with a positive correlation in both modalities were eligible for the next step.

In a second step, we used Bayes factors [53,54] to determine the flipping point where modality became obsolete as explanatory variable. Bayes factors express the ratio of the marginal likelihood of the data under the compared models; since they consider the number of free parameters, they allow for the selection of the "better" model (best fit to the data and most parsimonious). For every session, we obtained the mean SCR (log-transformed and normalized values) for both modalities; sessions with the largest predominance of heat-SCR were then consecutively removed. After each removal, we obtained the Bayes factors for the remaining sample, comparing the model with intensity only as predictor to that with modality added as predictor. Once the Bayes factor dropped below 1 (meaning that the addition of modality as predictor did not serve to improve the model), we stopped the pruning procedure. This relatively permissive criterion for session inclusion was chosen in order to preserve as many sessions as possible.

This procedure yielded a sample where modality did not contribute to explaining the SCR data (as indicated by recalculating the random intercept model described under "Skin conductance results"), with 26 unique subjects contributing 33 sessions. From the first cohort, 15 subjects contributed 19 sessions, from the second cohort, 11 subjects contributed 13 sessions to the SCR-equalized analysis.

bioRxiv preprint doi: https://doi.org/10.1101/581504; this version posted March 18, 2019. The copyright holder for this preprint (which was not certified by peer review) is the author/funder, who has granted bioRxiv a license to display the preprint in perpetuity. It is made available under aCC-BY 4.0 International license.

588 *Differences between first and second cohort*

589 Since we had determined that not every person's skin conductance responded to both modalities to
590 a comparable extent, we set out to select a subsample of persons who had comparable SCR. To reach
591 a sufficient number of such "responders", we had to perform an additional data collection.

592 Because of logistical reasons (scanner upgrade in January 2018), some parameters of fMRI
593 acquisition had to be modified for the new PRISMA 3T MR Scanner (Siemens, Erlangen, Germany).
594 Instead of a 12-channel head coil, we had to employ a 20-channel head coil. Delivery of the auditory
595 stimulus was performed with a CONFON headphone (Cambridge Research Systems Ltd, Rochester,
596 United Kingdom). These measures necessitated the exclusion of subjects with head circumference
597 above 60cm.

598 Furthermore, to facilitate increased SCR responding to sound, we increased the amplitude of the
599 sound stimuli. Using calibration data from the first data collection and linear extrapolation, we
600 calculated sound VAS targets required to induce SCRs of an amplitude comparable to those of heat
601 VAS targets of the same intended intensity 1 through 6. We determined that corresponding to our
602 heat VAS targets of 25, 35, 45, 55, 65, 75 (see "Heat stimuli and calibration"), we would need to apply
603 sound amplitudes inducing sound VAS targets of 48, 59, 70, 82, 93, 105. Furthermore, during subject
604 instruction, we emphasized the fact that the amplitude of sound stimuli was not within pathological
605 range. This was done to prevent overly cautious subject behavior, following anecdotal evidence from
606 the first cohort that sound stimuli were associated with higher safety concerns than heat stimuli.

607

608 *Statistical analyses*

609 All analyses were performed using MATLAB (version R2017b) and SPM12 (version 6906).

610 Significance level was set to $p=0.05$ for psychophysiological and behavioral data, whereas imaging
611 results were corrected using family-wise error rate adjustment at $p<0.05$. For visualization,

bioRxiv preprint doi: https://doi.org/10.1101/581504; this version posted March 18, 2019. The copyright holder for this preprint (which was not certified by peer review) is the author/funder, who has granted bioRxiv a license to display the preprint in perpetuity. It is made available under aCC-BY 4.0 International license.

612 activations are thresholded at p(uncorrected)<0.001 and overlaid on an average brain surface. All
613 coordinates are reported in Montreal Neurological Institute (MNI) space.

614 Skin conductance data and behavioral ratings were analyzed using linear mixed models with random
615 intercepts [55], with centering of predictors following recommendations [56].

616 Group-level analyses of imaging data were performed as within-subjects ANOVA (cf. “Analysis of
617 imaging data” above, and the respective Results sections).

618

619 **Acknowledgements**

620 This work was supported by European Research Council Advanced Grant ERC-2010-AdG_20100407
621 and Deutsche Forschungsgemeinschaft Grant SFB 936 Project A06. Björn Horing was supported by
622 the Alexander von Humboldt-Foundation (Feodor Lynen Return Fellowship). We thank Jürgen
623 Finsterbusch, Katrin Bergholz, Waldemar Schwarz and Kathrin Wendt for technical assistance during
624 MR data collection, and Lara Austermann, Tim Dretzler, Katharina Ebel and Matthias Kerkemeyer for
625 their assistance with data collection, and finally Christian Gaser for helpful comments concerning the
626 CAT12 toolbox.

627

628 **Conflicts of interest**

629 The authors declare no conflict of interest.

630

631 **Corresponding author**

632 Correspondence should be addressed to Dr. Björn Horing, Department of Systems Neuroscience,
633 University Medical Center Hamburg-Eppendorf, Martinistrasse 52, 20246 Hamburg, Germany.
634 b.horing@uke.de

bioRxiv preprint doi: https://doi.org/10.1101/581504; this version posted March 18, 2019. The copyright holder for this preprint (which was not certified by peer review) is the author/funder, who has granted bioRxiv a license to display the preprint in perpetuity. It is made available under aCC-BY 4.0 International license.

635 **References**

636 1. Moayedi M, Davis KD. Theories of pain: from specificity to gate control. J Neurophysiol.
637 2013;109(1):5–12. doi: 10.1152/jn.00457.2012

638 2. International Association for the Study of Pain (IASP). Pain terms: a list with definitions and
639 notes on usage. Recommended by the IASP Subcommittee on Taxonomy. Pain. 1979;6(3):249.

640 3. Tracey I, Mantyh PW. The cerebral signature for pain perception and its modulation. Neuron.
641 2007;55(3):377–91. doi: 10.1016/j.neuron.2007.07.012

642 4. Garcia-Larrea L, Peyron R. Pain matrices and neuropathic pain matrices: A review. Pain.
643 2013;154:S29–43. doi: 10.1016/j.pain.2013.09.001

644 5. Mouraux A, Diukova A, Lee MC, Wise RG, Iannetti GD. A multisensory investigation of the
645 functional significance of the “pain matrix.” Neuroimage. 2011;54(3):2237–49. doi:
646 10.1016/j.neuroimage.2010.09.084

647 6. Legrain V, Iannetti GD, Plaghki L, Mouraux A. The pain matrix reloaded: A salience detection
648 system for the body. Prog Neurobiol. 2011;93(1):111–24. doi:
649 10.1016/j.pneurobio.2010.10.005

650 7. Davis KD, Bushnell MC, Iannetti GD, St Lawrence K, Coghill R. Evidence against pain specificity
651 in the dorsal posterior insula. F1000Research. 2015;4(2):362. doi:
652 10.12688/f1000research.6833.1

653 8. Salomons T V., Iannetti GD, Liang M, Wood JN. The “pain matrix” in pain-free individuals.
654 JAMA Neurol. 2016;73(6):4–5. doi: 10.1001/jamaneurol.2016.0653

655 9. Segerdahl AR, Mezue M, Okell TW, Farrar JT, Tracey I. The dorsal posterior insula subserves a
656 fundamental role in human pain. Nat Neurosci. 2015;18(4):499–500. doi: 10.1038/nn.3969

657 10. Mouraux A, Iannetti GD. The search for pain biomarkers in the human brain. Brain.

bioRxiv preprint doi: https://doi.org/10.1101/581504; this version posted March 18, 2019. The copyright holder for this preprint (which was not certified by peer review) is the author/funder, who has granted bioRxiv a license to display the preprint in perpetuity. It is made available under aCC-BY 4.0 International license.

2018;141(12):3290–307. doi: 10.1093/brain/awy281

11. Büchel C, Geuter S, Sprenger C. Comparing Painful Stimulation vs Rest in Studies of Pain. JAMA Neurol. 2016;73(10):1258. doi: 10.1001/jamaneurol.2016.2989

12. Bornhövd K, Quante M, Glauche V, Bromm B, Weiller C, Büchel C. Painful stimuli evoke different stimulus-response functions in the amygdala, prefrontal, insula and somatosensory cortex: a single-trial fMRI study. Brain. 2002;125(Pt 6):1326–36.

13. Loggia ML, Edwards RR, Kim J, Vangel MG, Wasan AD, Gollub RL, et al. Disentangling linear and nonlinear brain responses to evoked deep tissue pain. Pain. 2012;153(10):2140–51. doi: 10.1016/j.pain.2012.07.014

14. Tiemann L, Hohn VD, Ta Dinh S, May ES, Nickel MM, Gross J, et al. Distinct patterns of brain activity mediate perceptual and motor and autonomic responses to noxious stimuli. Nat Commun. 2018;9(1):4487. doi: 10.1038/s41467-018-06875-x

15. Boucsein W. Electrodermal activity. 2nd ed. New York: Springer; 2012.

16. Bastuji H, Frot M, Perchet C, Hagiwara K, Garcia-Larrea L. Convergence of sensory and limbic noxious input into the anterior insula and the emergence of pain from nociception. Sci Rep. 2018;8(1):13360. doi: 10.1038/s41598-018-31781-z

17. Bastuji H, Frot M, Perchet C, Magnin M, Garcia-Larrea L. Pain networks from the inside: Spatiotemporal analysis of brain responses leading from nociception to conscious perception. Hum Brain Mapp. 2016;37(12):4301–15. doi: 10.1002/hbm.23310

18. Pomares FB, Faillenot I, Barral FG, Peyron R. The “where” and the “when” of the BOLD response to pain in the insular cortex. Discussion on amplitudes and latencies. Neuroimage. 2013;64:466–75. doi: 10.1016/j.neuroimage.2012.09.038

19. Roy M, Shohamy D, Daw N, Jepma M, Wimmer GE, Wager TD. Representation of aversive prediction errors in the human periaqueductal gray. Nat Neurosci. 2014;17(11):1607–12. doi:

bioRxiv preprint doi: https://doi.org/10.1101/581504; this version posted March 18, 2019. The copyright holder for this preprint (which was not certified by peer review) is the author/funder, who has granted bioRxiv a license to display the preprint in perpetuity. It is made available under aCC-BY 4.0 International license.

682 10.1038/nn.3832

683 20. D'Hondt F, Lassonde M, Collignon O, Dubarry A-S, Robert M, Rigoulot S, et al. Early brain-body
684 impact of emotional arousal. Front Hum Neurosci. 2010;4:33. doi:
685 10.3389/fnhum.2010.00033

686 21. Bradley MM, Codispoti M, Cuthbert BN, Lang PJ. Emotion and motivation I: Defensive and
687 appetitive reactions in picture processing. Emotion. 2001;1(3):276–98. doi: 10.1037/1528-
688 3542.1.3.276

689 22. Kayser C, Petkov CI, Lippert M, Logothetis NK. Mechanisms for Allocating Auditory Attention:
690 An Auditory Saliency Map. Curr Biol. 2005;15(21):1943–7. doi: 10.1016/j.cub.2005.09.040

691 23. Baliki MN, Geha PY, Apkarian A V. Parsing pain perception between nociceptive
692 representation and magnitude estimation. J Neurophysiol. 2009;101(2):875–87. doi:
693 10.1152/jn.91100.2008

694 24. Hutchison JL, Hubbard NA, Brigante RM, Turner M, Sandoval TI, Hillis GAJ, et al. The efficiency
695 of fMRI region of interest analysis methods for detecting group differences. J Neurosci
696 Methods. 2014;226:57–65. doi: 10.1016/j.jneumeth.2014.01.012

697 25. Geuter S, Boll S, Eippert F, Büchel C. Functional dissociation of stimulus intensity encoding and
698 predictive coding of pain in the insula. Elife. 2017;6. doi: 10.7554/eLife.24770

699 26. Moayedi M, Weissman-Fogel I. Is the insula the "how much" intensity coder? J Neurophysiol.
700 2009;102(3):1345–7. doi: 10.1152/jn.00356.2009

701 27. Taylor KS, Seminowicz DA, Davis KD. Two systems of resting state connectivity between the
702 insula and cingulate cortex. Hum Brain Mapp. 2009;30(9):2731–45. doi: 10.1002/hbm.20705

703 28. Eckert MA, Menon V, Walczak A, Ahlstrom J, Denslow S, Horwitz A, et al. At the heart of the
704 ventral attention system: the right anterior insula. Hum Brain Mapp. 2009;30(8):2530–41. doi:
705 10.1002/hbm.20688

bioRxiv preprint doi: https://doi.org/10.1101/581504; this version posted March 18, 2019. The copyright holder for this preprint (which was not certified by peer review) is the author/funder, who has granted bioRxiv a license to display the preprint in perpetuity. It is made available under aCC-BY 4.0 International license.

706 29. Mazzola L, Isnard J, Peyron R, Mauguière F. Stimulation of the human cortex and the
707 experience of pain: Wilder Penfield's observations revisited. Brain. 2012;135(2):631–40. doi:
708 10.1093/brain/awr265

709 30. Mazzola L, Faillenot I, Barral F-G, Mauguière F, Peyron R. Spatial segregation of somato-
710 sensory and pain activations in the human operculo-insular cortex. Neuroimage.
711 2012;60(1):409–18. doi: 10.1016/j.neuroimage.2011.12.072

712 31. Ostrowsky K, Magnin M, Ryvlin P, Isnard J, Guenot M, Mauguière F. Representation of pain
713 and somatic sensation in the human insula: a study of responses to direct electrical cortical
714 stimulation. Cereb Cortex. 2002;12(4):376–85.

715 32. Garcia-Larrea L, Mauguière F. Pain syndromes and the parietal lobe. In: Handbook of Clinical
716 Neurology. 2018 [cited 2019 Jan 18]. p. 207–23. doi: 10.1016/B978-0-444-63622-5.00010-3

717 33. Liberati G, Klöcker A, Safronova MM, Ferrão Santos S, Ribeiro Vaz J-G, Raftopoulos C, et al.
718 Nociceptive Local Field Potentials Recorded from the Human Insula Are Not Specific for
719 Nociception. Apkarian AV, editor. PLOS Biol. 2016;14(1):e1002345. doi:
720 10.1371/journal.pbio.1002345

721 34. Baliki MN, Geha PY, Fields HL, Apkarian AV. Predicting value of pain and analgesia: Nucleus
722 accumbens response to noxious stimuli changes in the presence of chronic pain. Neuron.
723 2010;66(1):149–60. doi: 10.1016/j.neuron.2010.03.002

724 35. Price DD, McGrath PA, Rafii A, Buckingham B. The validation of visual analogue scales as ratio
725 scale measures for chronic and experimental pain. Pain. 1983;17(1):45–56. doi:
726 10.1016/0304-3959(83)90126-4

727 36. Duncan GH, Bushnell CM, Lavigne GJ. Comparison of verbal and visual analogue scales for
728 measuring the intensity and unpleasantness of experimental pain. Pain. 1989;37(3):295–303.
729 doi: 10.1016/0304-3959(89)90194-2

bioRxiv preprint doi: https://doi.org/10.1101/581504; this version posted March 18, 2019. The copyright holder for this preprint (which was not certified by peer review) is the author/funder, who has granted bioRxiv a license to display the preprint in perpetuity. It is made available under aCC-BY 4.0 International license.

730 37. Quiton RL, Greenspan JD. Across- and within-session variability of ratings of painful contact
731 heat stimuli. Pain. 2008;137(2):245–56. doi: 10.1016/j.pain.2007.08.034

732 38. Lashkari D, Vul E, Kanwisher N, Golland P. Discovering structure in the space of fMRI
733 selectivity profiles. Neuroimage. 2010;50(3):1085–98. doi: 10.1016/j.neuroimage.2009.12.106

734 39. Kanwisher N. Functional specificity in the human brain: A window into the functional
735 architecture of the mind. Proc Natl Acad Sci. 2010;107(25):11163–70. doi:
736 10.1073/pnas.1005062107

737 40. Beck AT, Steer RA, Brown GK. Manual for the Beck Depression Inventory-II. San Antonio, TX:
738 Psychological Corporation Press; 1996.

739 41. Kroenke K, Spitzer RL, Williams JBW. The PHQ-15: validity of a new measure for evaluating the
740 severity of somatic symptoms. Psychosom Med. 2002;64(2):258–66.

741 42. Benedek M, Kaernbach C. A continuous measure of phasic electrodermal activity. J Neurosci
742 Methods. 2010;190(1):80–91. doi: 10.1016/J.JNEUMETH.2010.04.028

743 43. Geuter S, Gamer M, Onat S, Büchel C. Parametric trial-by-trial prediction of pain by easily
744 available physiological measures. Pain. 2014;155(5):994–1001. doi:
745 10.1016/j.pain.2014.02.005

746 44. Loggia ML, Juneau M, Bushnell MC. Autonomic responses to heat pain: Heart rate, skin
747 conductance, and their relation to verbal ratings and stimulus intensity. Pain.
748 2011;152(3):592–8. doi: 10.1016/j.pain.2010.11.032

749 45. Bach DR, Flandin G, Friston KJ, Dolan RJ. Modelling event-related skin conductance responses.
750 Int J Psychophysiol. 2010;75(3):349–56. doi: 10.1016/J.IJPSYCHO.2010.01.005

751 46. Coghill RC, Sang CN, Maisog JM, Iadarola MJ. Pain Intensity Processing Within the Human
752 Brain: A Bilateral, Distributed Mechanism. J Neurophysiol. 1999;82(4):1934–43. doi:
753 10.1152/jn.1999.82.4.1934

bioRxiv preprint doi: https://doi.org/10.1101/581504; this version posted March 18, 2019. The copyright holder for this preprint (which was not certified by peer review) is the author/funder, who has granted bioRxiv a license to display the preprint in perpetuity. It is made available under aCC-BY 4.0 International license.

754 47. Eickhoff SB, Stephan KE, Mohlberg H, Grefkes C, Fink GR, Amunts K, et al. A new SPM toolbox
755 for combining probabilistic cytoarchitectonic maps and functional imaging data. Neuroimage.
756 2005;25(4):1325–35. doi: 10.1016/J.NEUROIMAGE.2004.12.034

757 48. Rolke R, Magerl W, Campbell KA, Schalber C, Caspari S, Birklein F, et al. Quantitative sensory
758 testing: A comprehensive protocol for clinical trials. Eur J Pain. 2006;10(1):77–88. doi:
759 10.1016/j.ejpain.2005.02.003

760 49. Ellerbrock I, May A. MRI scanner environment increases pain perception in a standardized
761 nociceptive paradigm. Brain Imaging Behav. 2015;9(4):848–53. doi: 10.1007/s11682-014-
762 9345-5

763 50. Awiszus F. TMS and threshold hunting. Suppl Clin Neurophysiol. 2003;56:13–23. doi:
764 10.1016/S1567-424X(09)70205-3

765 51. Hall DA, Summerfield AQ, Gonçalves MS, Foster JR, Palmer AR, Bowtell RW. Time-course of
766 the auditory BOLD response to scanner noise. Magn Reson Med. 2000;43(4):601–6.

767 52. National Institute for Occupational Safety and Health (NIOSH). Criteria for a Recommended
768 Standard: Occupational Noise Exposure. Revised Criteria [Internet]. 1998.

769 53. Kass RE, Raftery AE. Bayes Factors. J Am Stat Assoc. 1995;90(430):773–95. doi:
770 10.1080/01621459.1995.10476572

771 54. Rouder JN, Morey RD. Default Bayes Factors for model selection in regression. Multivariate
772 Behav Res. 2012;47(6):877–903. doi: 10.1080/00273171.2012.734737

773 55. Raudenbush SW, Bryk AS. Hierarchical linear models: Applications and data analysis.
774 Thousand Oaks, CA: Sage; 2002.

775 56. Hofmann DA, Gavin MB. Centering decisions in Hierarchical Linear Models: Implications for
776 research in organizations. J Manage. 1998;24(5):623–41. doi: 10.1177/014920639802400504

bioRxiv preprint doi: https://doi.org/10.1101/581504; this version posted March 18, 2019. The copyright holder for this preprint (which was not certified by peer review) is the author/funder, who has granted bioRxiv a license to display the preprint in perpetuity. It is made available under aCC-BY 4.0 International license.

777 # Supporting information

778

779 **S1 Table**. Sample descriptive statistics.

| Questionnaire | Construct | Mean±SD | Sample range | Possible range |
|---|---|---|---|---|
| **BDI-II** [SR 1,2] | Depression | 2.0±2.2 | 0-8 | 0-63 |
| **PHQ15** [SR 3] | Somatization | 3.9±2.3 | 0-9 | 0-30 |
| **FPQ** [SR 4] | | | | |
| severe | Fear of pain | 28.9±8.3 | 11-42 | 10-50 |
| minor | Fear of pain | 14.0±4.5 | 10-27 | 10-50 |
| **PVAQ** [SR 5] | Pain vigilance and awareness | 34.6±8.7 | 21-54 | 0-80 |
| **PSQ** [SR 6] | Pain sensitivity | 45.1±14.8 | 17-73 | 0-140 |
| **PRSS** [SR 7] | | | | |
| Catastrophizing | Pain catastrophizing | 8.6±5.4 | 2-21 | 0-45, higher more catastrophizing |
| Coping | Pain coping | 29.8±5.2 | 19-38 | 0-45, higher more active coping |
| **STAI** [SR 8,9] | | | | |
| Trait | Trait anxiety | 32.0±6.9 | 21-49 | 20-80 |
| State | State anxiety (pre experiment) | 31.5±6.2 | 22-51 | 20-80 |
| **MDMQ** [SR 10] | | | | |
| GoodBad A | Mood: Good vs bad (pre exp.) | 17.7±1.9 | 12-20 | 4-24, the higher the better |
| AwakeTired A | Mood: Awake vs tired (pre exp.) | 15.2±2.9 | 8-19 | 4-24, the higher the more awake |

bioRxiv preprint doi: https://doi.org/10.1101/581504; this version posted March 18, 2019. The copyright holder for this preprint (which was not certified by peer review) is the author/funder, who has granted bioRxiv a license to display the preprint in perpetuity. It is made available under aCC-BY 4.0 International license.

| | | | | |
|---|---|---|---|---|
| CalmNervous A | Mood: Calm vs nervous (post exp.) | 16.5±2.6 | 10-20 | 4-24, the higher the calmer |
| GoodBad B | Mood: Good vs bad (pre exp.) | 17.2±1.7 | 12-19 | 4-24, the higher the better |
| AwakeTired B | Mood: Awake vs tired (pre exp.) | 10.1±2.4 | 6-16 | 4-24, the higher the more awake |
| CalmNervous B | Mood: Calm vs nervous (post exp.) | 17.2±2.1 | 12-20 | 4-24, the higher the calmer |

780

781

bioRxiv preprint doi: https://doi.org/10.1101/581504; this version posted March 18, 2019. The copyright holder for this preprint (which was not certified by peer review) is the author/funder, who has granted bioRxiv a license to display the preprint in perpetuity. It is made available under aCC-BY 4.0 International license.

782 **S2 Table**. Average calibrated sound intensities 1 through 6, which were used as stimuli during the experiment.

783 Cohort 2 received higher intensities, see Methods for rationale.

| | **Cohort 1 (n=15)** | | | **Cohort 2 (n=11)** | | |
|---|---|---|---|---|---|---|
| **Intensity** | **Target VAS** | **dBA mean±SD** | **Range** | **Target VAS** | **dBA mean±SD** | **Range** |
| 1 | 25 | 70.5±7.4 | 57.7-82.9 | 48 | 86.1±5.9 | 77.8-99.3 |
| 2 | 35 | 74.2±6.6 | 62.4-85.9 | 59 | 92.2±5.9 | 81.2-101.5 |
| 3 | 45 | 77.9±6.0 | 67.2-88.7 | 70 | 95.6±6.0 | 84.4-102.5 |
| 4 | 55 | 81.4±5.5 | 70.8-91.2 | 82 | 97.7±5.0 | 87.7-103.0 |
| 5 | 65 | 84.8±5.3 | 74.3-93.4 | 93 | 99.1±3.9 | 90.5-103.0 |
| 6 | 75 | 87.8±5.2 | 77.8-95.3 | 105 | 100.3±3.0 | 93.3-103.0 |

784

785

bioRxiv preprint doi: https://doi.org/10.1101/581504; this version posted March 18, 2019. The copyright holder for this preprint (which was not certified by peer review) is the author/funder, who has granted bioRxiv a license to display the preprint in perpetuity. It is made available under aCC-BY 4.0 International license.

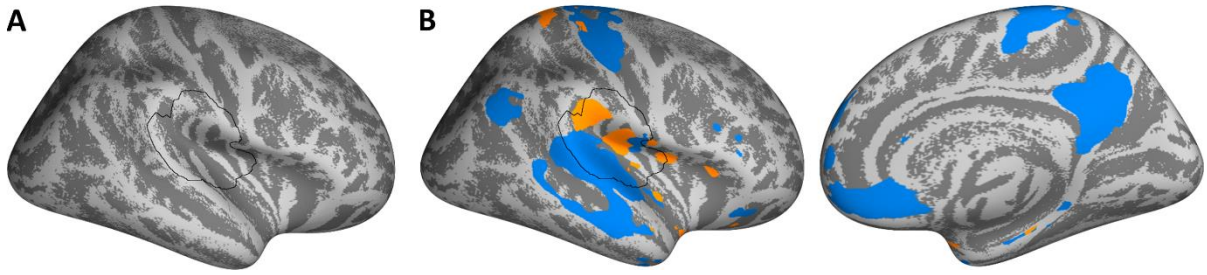


**S1 Figure**. Binary and signed masks used for analyses. **A.** Binary mask used for small volume correction used for all analyses (unless otherwise noted), delineated by the black line. **B.** Signed mask used for covering heat (orange) or sound (blue) contrasts.

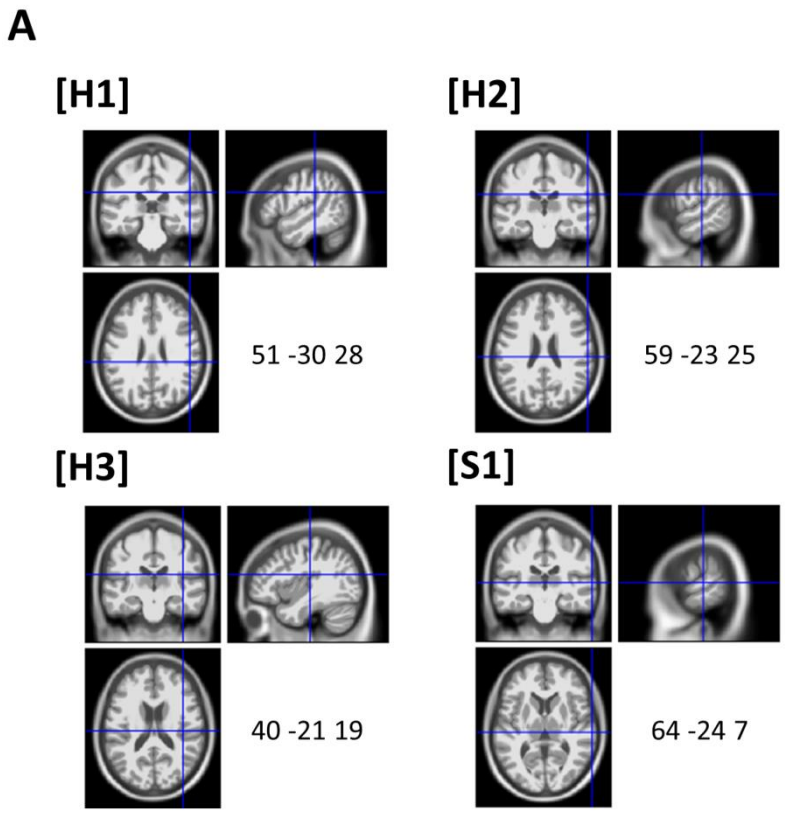


**S2 Figure**. Location of peak voxels for modality main effects (H1 through H3 for heat, S1 for sound). Also see Figure 4.

bioRxiv preprint doi: https://doi.org/10.1101/581504; this version posted March 18, 2019. The copyright holder for this preprint (which was not certified by peer review) is the author/funder, who has granted bioRxiv a license to display the preprint in perpetuity. It is made available under aCC-BY 4.0 International license.

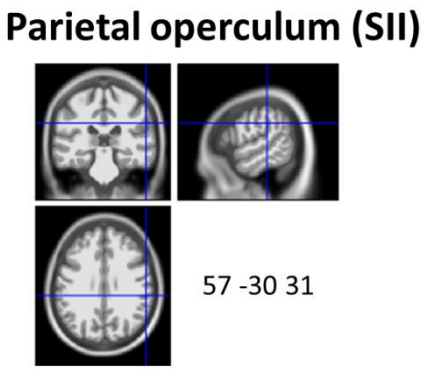


797

798 **S3 Figure**. Location of peak voxel for parametric modulation by heat intensity. Also see Figure 5.

799

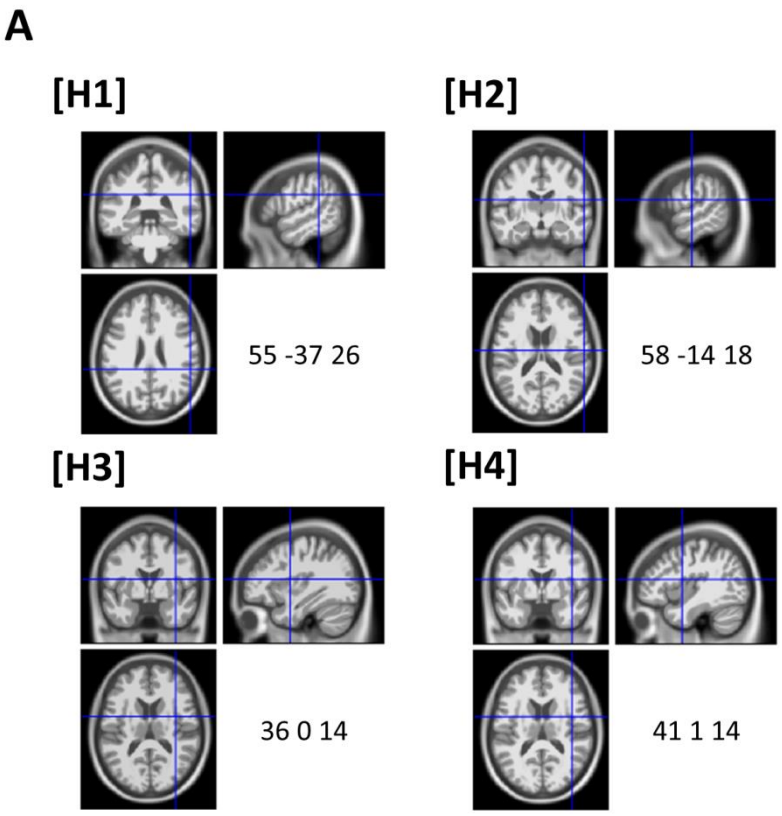


800

801 **S4 Figure**. Location of peak voxels for parametric modulation by ratings (H1 through H4). Also see Figure 6.

802

803

804

bioRxiv preprint doi: https://doi.org/10.1101/581504; this version posted March 18, 2019. The copyright holder for this preprint (which was not certified by peer review) is the author/funder, who has granted bioRxiv a license to display the preprint in perpetuity. It is made available under aCC-BY 4.0 International license.

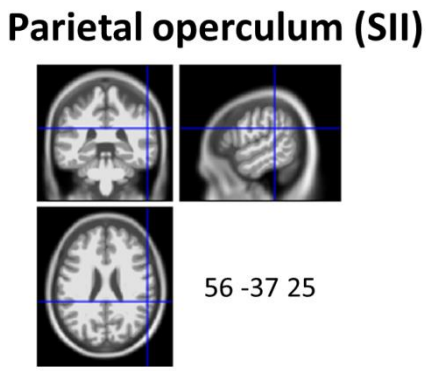


805

806 **S5 Figure**. Location of peak voxel for activation corresponding to the three axioms. Also see Figure 7.

807

808

bioRxiv preprint doi: https://doi.org/10.1101/581504; this version posted March 18, 2019. The copyright holder for this preprint (which was not certified by peer review) is the author/funder, who has granted bioRxiv a license to display the preprint in perpetuity. It is made available under aCC-BY 4.0 International license.

809 **Supporting information – References**

810 SR 1. Beck AT, Steer RA, Brown GK. Manual for the Beck Depression Inventory-II. San Antonio, TX:
811 Psychological Corporation Press; 1996.

812 SR 2. Hautzinger M, Keller F, Kühner C. BDI-II. Beck-Depressions-Inventar. Revision. 2nd ed.
813 Frankfurt: Pearson Assessment; 2009.

814 SR 3. Kroenke K, Spitzer RL, Williams JBW. The PHQ-15: validity of a new measure for evaluating the
815 severity of somatic symptoms. Psychosom Med. 2002;64(2):258–66.

816 SR 4. McNeil DW, Rainwater AJ. Development of the Fear of Pain Questionnaire-III. J Behav Med.
817 1998;21(4):389–410.

818 SR 5. McCracken LM. "Attention" to pain in persons with chronic pain: A behavioral approach.
819 Behav Ther. 1997;28(2):271–84. doi: 10.1016/S0005-7894(97)80047-0

820 SR 6. Ruscheweyh R, Marziniak M, Stumpenhorst F, Reinholz J, Knecht S. Pain sensitivity can be
821 assessed by self-rating: Development and validation of the Pain Sensitivity Questionnaire.
822 Pain. 2009;146(1):65–74. doi: 10.1016/j.pain.2009.06.020

823 SR 7. Flor H, Behle DJ, Birbaumer N. Assessment of pain-related cognitions in chronic pain patients.
824 Behav Res Ther. 1993;31(1):63–73.

825 SR 8. Spielberger CD, Gorsuch RL, Lushene RE. Manual for the State-Trait Anxiety Inventory. Palo
826 Alto, CA: Consulting Psychologists Press; 1970.

827 SR 9. Laux L, Glanzmann P, Schaffner P, Spielberger CD. Das State-Trait-Angstinventar. Weinheim:
828 Beltz; 1981.

829 SR 10. Steyer R, Schwenkmezger P, Notz P, Eid M. Der Mehrdimensionale Befindlichkeitsfragebogen
830 (MDBF). Handanweisung. Göttingen: Hogrefe; 1997.

831